1979

Paleoclimatic Implications of Oxygen Isotope and Sedimentological Study of Late Miocene and Early Pliocene Sediments from the South Atlantic, Western Indian Ocean, and the Gulf of Aden

Kathryn M. Scanlon
University at Albany, State University of New York

Paleoclimatic Implications of Oxygen Isotope and Sedimentological Study of Late Miocene and Early Pliocene Sediments from the South Atlantic, Western Indian Ocean, and the Gulf of Aden

A thesis presented to the Faculty
of the State University of New York
at Albany
in partial fulfillment of the requirements
for the degree of
Master of Science

Department of Geological Sciences

Kathryn M. Scanlon

1979

ABSTRACT

Previous work by many authors has implied that the Antarctic ice sheet underwent a major expansion in the latest Miocene. It was intended in the present study to use the oxygen isotope event, which could be expected to accompany this glacial expansion, as a stratigraphic marker to aid in the correlation of several DSDP Sites. Samples were taken at approximately 100,000 year intervals throughout the latest Miocene and early Pliocene sections at Sites 237 and 249 in the western Indian Ocean, Site 360 in the South Atlantic and Site 231 in the Gulf of Aden. Oxygen isotope analyses were done on bulk samples of juvenile planktonic foraminifera and calcium carbonate analyses, size separations, and dissolution/fragmentation studies were done by conventional techniques.

A cool period is recognized between about 5.7 m.y. and 4.9 m.y. at all four sites, but it is not consistently observed in the oxygen isotope records from these sites. This implies that the latest Miocene expansion of the Antarctic ice sheet did not produce an oxygen isotopic anomaly of sufficient magnitude to be a reliable world-wide stratigraphic marker. Attempts to correlate sedimentologic events between sites have revealed that the biostratigraphy currently available in the Initial Reports of the Deep Sea Drilling Project for the late Miocene and early Pliocene is not precise to more than about 300,000 years.

Department of Geological Sciences
State University of New York at Albany
1400 Washington Avenue
Albany, N. Y. 12222

State University of New York at Albany

Department of Geological Sciences

The thesis for the master's degree submitted by

Kathryn M. Scanlon

under the title

Paleoclimatic Implications of Oxygen Isotope and Sedimentological Study of Late Miocene and Early Pliocene Sediments from the South Atlantic, Western Indian Ocean and the Gulf of Aden

has been read by the undersigned. It is hereby recommended for acceptance by the Faculty with credit to the amount of six semester hours.

(Signed) _____

(Date) _____

(Signed) _____

(Date) _____

Recommendation accepted by the Dean of Graduate Studies for the Graduate Academic Council.

(Signed) _____

(Date) _____

"He had long ago decided, since he was a serious scholar, that the caves of ocean bear no gems, but only soggy glub and great gobs of mucky gump."

James Thurber

ACKNOWLEDGMENTS

Many people at Lamont-Doherty Geological Observatory gave freely of their time, equipment and expertise. Outstanding among these is P. Gibson, who ran the mass spectrometer for most of the oxygen isotope analyses, generously contributing many hours of her own time. O. Anderson, J. Durazzi, J. Lawrence, A. Sotiropoulos, P. Thompson and J. Wollin (all at Lamont-Doherty Geological Observatory) and D. Kelly (at State University of New York at Albany) are thanked for their help.

W.S.F. Kidd (S.U.N.Y.A.), P.J. Fox (S.U.N.Y.A.), and W.B.F. Ryan (L.D.G.O.) read various drafts of this thesis and made valuable suggestions. I am particularly indebted to W.B.F. Ryan and P.J. Fox for their advice, guidance and encouragement through all stages of this thesis.

Samples were obtained through the courtesy of the Deep Sea Drilling Project and the National Science Foundation. Partial support for this work was provided by N.S.F. Grant No. OCE 76-21964. The remainder of the support for this work was largely of the moral variety, and was amply supplied by the residents of the Green Barn, my parents and E.J. Rosencrantz.

TABLE OF CONTENTS

LIST OF TABLES

LIST OF FIGURES

INTRODUCTION

Oxygen isotope work done by Shackleton and Kennett (1975a and 1975b) and Kennett, et al. (1979) on forams from Sites 281 and 284 of the Deep Sea Drilling Project (DSDP) in the Tasman Sea revealed a positive pulse in ^{18}O content in the latest Miocene and earliest Pliocene. The signal was interpreted as an increase by 50 per cent of the Antarctic ice sheet (relative to present Antarctic ice volume). Such an increase in ice volume implies a sea level drop of roughly 40 to 70 meters (Adams, et al., 1977 and Shackleton and Kennett, 1975b). Obviously a climatic event of this magnitude should be observable in deep sea sediments from all of the world's oceans and could be valuable as an isochronous stratigraphic marker.

An expansion of the Antarctic ice sheet during the latest Miocene is supported by observations made during DSDP Leg 28, in the Ross Sea (Hayes, Frakes, et al., 1975). The extent of ice rafted debris north of Antarctica and possible erosional evidence for bottom currents and grounded sea ice during the latest Miocene imply an expansion of Antarctic glaciation.

A late Miocene cooling event is compatible with observations in several disciplines. Polar microfaunal assemblages are observed in lower-than-normal latitudes (Ingle, 1978; Harper and Barron, 1978; Hayes and Frakes, et al., 1975; Shackleton and Kennett, 1975a and 1975b) during the

late Miocene and Southern Ocean planktonic foram assemblages show low diversity (Kennett, 1978). Changes are observed in the diversity of large land fauna approximately 5 to 6 m.y. ago (Van Couvering, 1978). Adams, et al. (1977) give several examples of late Miocene marine regressive sequences from various parts of the world.

Probably the most significant and interesting event that corresponds in time with the proposed late Miocene climatic deterioration is the deposition of a large volume of salt in the Mediterranean. The causes and mechanics of the Mediterranean "salinity crisis" are subjects of debate (Drooger, 1973 and Hsü, et al., 1977), but it is generally agreed that world-wide climatic fluctuations and Messinian[1]

---

[1]The term Messinian was first used in a stratigraphic sense by Charles Mayer (1867), but his usage was unclear and the term did not come into common usage until it was chosen by the Vienna Congress of the Committee on Mediterranean Neogene Stratigraphy as the final stage of the Miocene in the Mediterranean. After the Vienna Congress, Selli (1960) designated a composite type section for the Messinian Stage of the Miocene at Capodarso and Pasquasia in Sicily (there were no appropriate sections near Messina) that included the whole of the section with abnormal salinities (fresh to hypersaline) between the normal marine sediments of the Miocene and Pliocene.

Correlation of Messinian age events in the Mediterranean to events outside of the Mediterranean is fraught with difficulty (see, e.g., Berggren, 1973 and Rio, et al., 1977). It is generally agreed, however, that the base of the Messinian stage lies within Blow's (1969) foram zone N17 and within the calcareous nannoplankton zone NN11, while the end of the Messinian stage corresponds to the end of Blow's (1969) zone N17 and is within NN12. Ryan, et al. (1974) assign tentative ages of 6.6 m.y. and 5.2 m.y. to the lower and upper boundaries, respectively, of the Messinian stage on the basis of biostratigraphic and paleomagnetic correlations.

events in the Mediterranean are related. Ryan (1973) has suggested that a lowering of sea level related to an expansion of the Antarctic ice sheet could serve to isolate the Mediterranean from the World Ocean system, allowing it to dessicate. Alternatively, he suggests that the removal of a large amount of salt from the World Ocean (he estimates that 6 per cent of the salts dissolved in the Miocene World Ocean were deposited in the Mediterranean during the Messinian) could raise the freezing temperature sufficiently to significantly increase the areal extent of sea ice, which would increase the earth's albedo and perhaps begin a snowballing effect, resulting in a major glacial period. The relative timing of late Miocene events within and outside the Mediterranean, then, is very important for complete understanding of the "salinity crisis."

The purpose of the present study is to identify the late Miocene isotopic event by doing ^{18}O analyses of forams from several DSDP Sites. Using this event as a stratigraphic marker, it would be possible to correlate data from other paleoenvironmental indicators ($\%CaCO_3$, grain size, dissolution and detrital mineralogy) and perhaps determine the sequence of climatic events in the latest Miocene relative to the Mediterranean "salinity crisis."

THE CORES

Cores from DSDP Sites 249 and 237 in the western Indian Ocean, Site 360 in the South Atlantic, and Site 231 in the Gulf of Aden (see Figure 1 and Table I for exact locations) were chosen for this study for several reasons. Most importantly, all have long, uninterrupted late Miocene to early Pliocene sections that were continuously cored with good recovery. Sedimentation rates during the late Miocene at these sites vary from 11 m/m.y. at Site 237 up to about 60 m/m.y. at Sites 249 and 360 (see Table I). The mean sedimentation rate at Site 360 is approximately 20 m/m.y., but it jumps to about 60 m/m.y. for a short time during the late Miocene (Bolli, Ryan, et al., 1978).

Other considerations in choosing the sites for this study were that the sediments should be primarily foram nanno ooze (see Figure 2) to ensure the availability of material for oxygen isotope analyses and that the water depth should be relatively shallow to minimize the effects of dissolution (see Table I).

In addition, there are no constraining sills or straits between the sites, making biostratigraphic correlations relatively straight-forward. The four sites are distributed through 45° of latitude which might allow the detection of a gradation of effects with latitude or of a time lag related to latitude.

Figure 1: Location map for DSDP Sites 231, 237, 249 and 360.

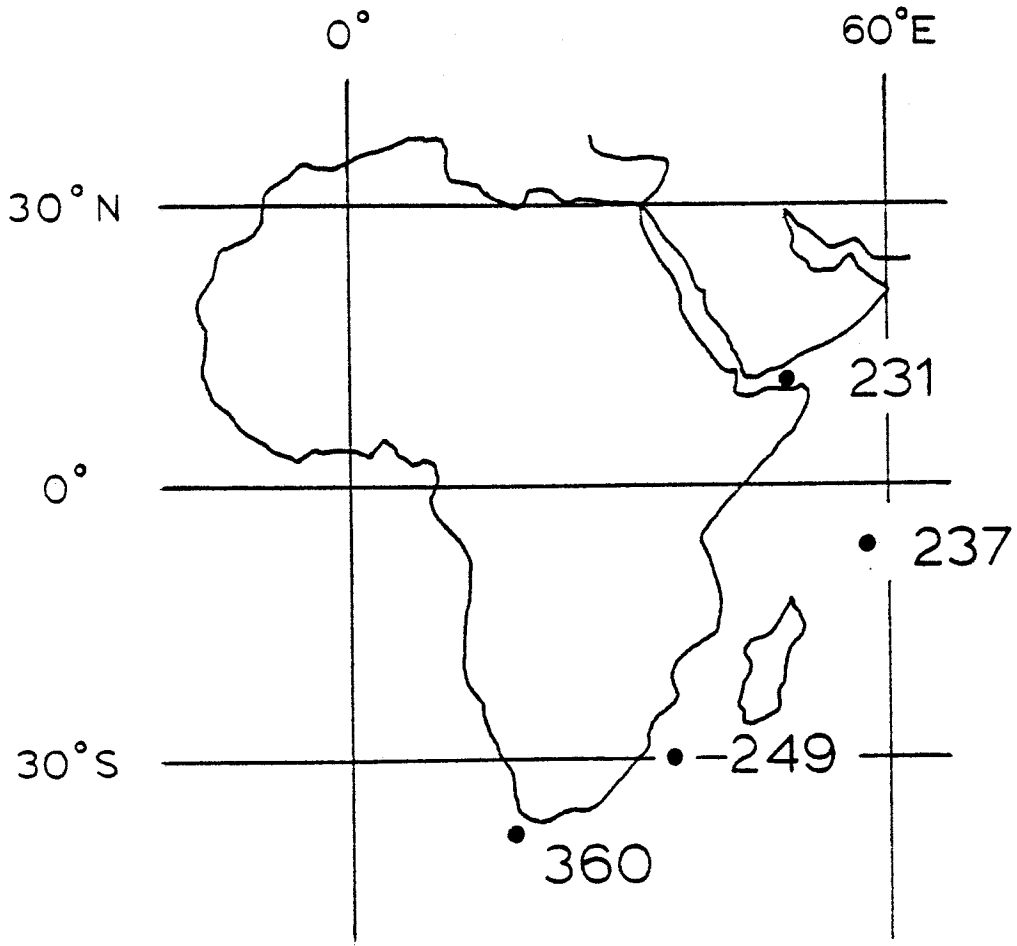
0°
60°E
30°N
231
0°
237
30°S
-249
360

TABLE I

SITE	231	237	249	360
LOCATION	Gulf of Aden	Mascarene Plateau NE of Madagascar	Mozambique Ridge	Upper cont. rise W of Cape Agulhas, S.A.
POSITION	$11^{o}53.41'N$ $48^{o}14.71'E$	$07^{o}04.99'S$ $58^{o}07.48'E$	$29^{o}56.99'S$ $36^{o}04.62'E$	$35^{o}50.75'S$ $18^{o}05.79'E$
WATER DEPTH	2152 meters	1623 meters	2088 meters	2949 meters
SED. RATE IN LATE MIO.	38 m/m.y.	7 to 24 m/m.y.	24 to 60 m/m.y.	20 to 60 m/m.y.

References: Sites 231 and 237: Fisher, Bunce, et al., 1974.

Site 249: Simpson, Schlick, et al., 1974.

Site 360: Bolli, Ryan, et al., 1978.

Site 360 (on the upper continental rise off South Africa) and Site 231 (in the Gulf of Aden) are sufficiently close to continental areas that they might be expected to show changes in terrigenous sediment input related to sea level changes. This is particularly true of the Gulf of Aden site since it is nearly surrounded by land masses.

The locations of the individual samples within the cores are shown in Figure 2, along with the lithology, biostratigraphy and ages of the latest Miocene to earliest Pliocene sections of the four sites in this study. The sample spacing averages about 1 sample/100,000 years. This sampling is two to ten times more dense than the sampling done for previous oxygen isotope work on late Miocene sediments (e.g., Douglas and Savin, 1973 and 1975; Shackleton and Kennett, 1975a and 1975b; Grazzini, 1977 ; and Kennett, et al., 1979).

EXPERIMENTAL TECHNIQUES

Calcium Carbonate Analyses

Determinations of the per cent $CaCO_3$ in bulk sediment samples from all four sites were made using an apparatus similar to that described by Hülsemann (1966). Samples were air dried, pulverized and oven dried, then placed in a dessicator to cool. A weighed amount of each cooled sample was completely reacted with 2 Normal hydrochloric acid. Sample size for Sites 237, 249 and 360 averaged 0.1 grams, while for Site 231 (which has a lower $\%CaCO_3$) between 0.15 and 0.20 grams of sample were used. The carbon dioxide released by the reaction

$$2HCl + CaCO_3 \rightarrow CaCl_2 + H_2O + CO_2\uparrow$$

was measured by the displacement of a column of mercury. The per cent of carbonate was then calculated using the following formula:

$$\%CaCO_3 = \frac{(BPRES - M)(VCO_2)(0.1603)}{(RTEM + 273.16)(SAMWT)}$$

where BPRES is barometric pressure (millimeters of mercury), M is the water vapor pressure (millimeters of mercury), VCO_2 is the volume of CO_2 produced by the reaction and measured by the displacement of the mercury column (milliliters), RTEM is the room temperature (^{o}C), and SAMWT is the weight of the sample (grams). The addition of 273.16 to RTEM converts the ^{o}C to absolute temperature and 0.1603 is a constant.

Standard samples consisting of 0.1 ± 0.0005 grams of analytical grade 100 per cent $CaCO_3$ were run before beginning analysis of the unknown samples and then after each five analyses. All standards yielded values of 100 ± 1.6% except those standards run with the samples from Site 360. These latter standards ranged between 95.74 per cent and 97.71 per cent. This was evidently due to a small amount of leakage in the apparatus.

Size Separations

Each sample (approximately 10 c.c.) was divided into three size fractions by sieving. After drying at room temperature and weighing each sample, standard wet sieving techniques (Folk, 1974) were used to separate the sand-sized grains from the silt- and clay-sized grains. The finer grained fractions were discarded and the coarser fractions were dried at room temperature and weighed. The coarser fractions were further divided by dry sieving with a 180μ sieve (or, in the case of Site 360 samples, 177μ). The wet sieving of the samples from Sites 231, 237 and 249 was done with a 74μ sieve, while for Site 360, a 62μ sieve was used.

To check the efficiency of the wet sieving technique, all samples from Site 231 were resieved (this time, dry) with the 74μ sieve. The weights of the >74μ size fractions were slightly lower after the second sieving, but the character of the %>74μ vs depth plot is unchanged (see

Appendix A).

Another check on the size separation technique was done to determine whether drying at room temperature allowed a significant amount of water to remain in the samples, thus changing the sample weights. Baking was found to reduce the weight of one sample by less than 2 per cent (see Appendix A). This is taken to be representative of all samples.

Fragmentation of Forams

The per cent of fragments of forams relative to the per cent of whole forams in the >74μ (or 62μ) <180μ (or 177μ) size fractions was determined for all samples from Sites 237, 249 and 360. This was accomplished by counting several hundred individual forams or fragments of forams in each sample along fixed lines in a micropaleontology tray under a reflected light microscope.

To check the reproducibility of the results, all samples from Site 249 were counted a second time. Of the fifteen samples eleven increased by between 1 and 6 percentage points, three decreased by between 1 and 3 percentage points, and one increased by 10 percentage points. The average of the first counts was 22.8% fragments while the second counts averaged 26.2% fragments. The general increase in the number of fragments counted is attributed to fracturing of forams during the additional handling. The per cent of fragments values reported here for Site 249

are the percentages determined after adding fragments from both counts.

Mineralogy

Percentages of various minerals in the samples were estimated visually by examining the >74μ (or 62μ)<180μ (or 177μ) size fractions under a reflecting light microscope.

Oxygen Isotope Analyses

The oxygen isotope analyses were done on bulk samples from the size fractions between 74μ (or 62μ) and 180μ (or 177μ). About 95 per cent to 100 per cent of the whole forams in this size fraction are juvenile planktonic forams. Emiliani (1971) has shown that juveniles of all planktonic foram species inhabit the same shallow depth range. This means that virtually all of the young forams in each 74μ (or 62μ) to 180μ (or 177μ) size fraction sample deposited their tests under the same conditions. These whole juvenile planktonic forams are mixed with varying percentages of fragments of larger forams (generally of the same species as the whole forams) and very minor amounts of benthic forams and mineral grains.

The $\partial^{18}O$ versus depth curves obtained by Emiliani (1977) for samples of a similar size fraction of Quaternary Caribbean sediment show the same trends as the $\partial^{18}O$ versus depth curves he obtained using samples of the planktonic foram Globigerinoides sacculifera from the same cores (Emiliani, 1966). The plots of the analyses done on the bulk samples

contain more "noise" than do the plots of the species-specific analyses, but events as small as 0.5 per mil are readily correlatable between the two sets of data. Oxygen isotope analyses done in this manner cannot be used quantitatively (e.g. for paleotemperature determinations), but they can provide valuable qualitative data for the correlations of isotopic events at least as small as 0.5 per mil.

Preparation of these samples for isotopic analysis consisted of three steps. First, the samples were roasted in vacuo at 375°C for one hour, to remove any organic contaminants. Second, 5 to 10 mg of each (cooled) sample was weighed out and placed in a reaction tube. Third, the samples were gently crushed with a glass rod to insure complete reaction with the phosphoric acid. Inspection under a microscope established that this size fraction was nearly devoid of impurities, and it was therefore deemed unnecessary to clean the sample ultrasonically prior to analysis.

All of the oxygen isotope analyses except those done on samples 11-1A, 11-1B, 11-2, 11-3A, 11-3B and 11-4 from Site 237 were done on the Lamont Nuclide 6 inch dual collecting gas mass spectrometer. The CO_2 gas was evolved on line by reacting the samples with 100% orthophosphoric acid in a hot box at 50°C. A secondary standard, Solenhofen limestone (NBS-20) was analysed with each sample, the data being later converted to per mil deviation from PDB for this report. A $\partial^{18}O$ value of -4.14 per mil and a $\partial^{13}C$ value of -1.06 per mil for NBS-20 relative to PDB were

assumed (Craig, 1957). Overall reproducibility of results is estimated to be about ±0.15 per mil on the basis of replicate analysis of Solenhofen limestone.

Samples 11-1A, 11-1B, 11-2, 11-3A, 11-3B and 11-4 from Site 237 were prepared for oxygen isotope analyses in the same manner as all of the other samples. The oxygen isotope analyses were done on the Lamont Micromass #903 triple collecting mass spectrometer. The CO_2 gas was evolved on a separate vacuum apparatus by reaction with 100% ortho-phosphoric acid and equilibrated to 25°C in a water bath. To make the data comparable to the data obtained from the samples run at 50°C, 1.07 was subtracted from the values vs PDB. A secondary standard of Bahama oolite powder was run with each sample, the data being later converted to per mil deviation from PDB for this report. A $\partial^{18}O$ value of -0.64 per mil and a $\partial^{13}C$ value of +4.52 per mil for the Bahama oolite powder standard relative to PDB were assumed. Overall reproducibility of results is estimated to be about ±0.10 per mil on the basis of replicate analyses of Solenhofen limestone.

BIOSTRATIGRAPHIC CORRELATIONS

In Figure 2, first and last appearance datums as determined by various authors are plotted along with the ages assigned to them. Because of inconsistancies between different authors in the defining and assigning of faunal zones, first appearance and last appearance datums are used for correlation between sites here.

Four datums were used to correlate the cores from the four sites. The first appearance of Ceratolithus rugosus is found at all four sites and is assigned an age of 4.5 m.y. by Ryan, et al. (1974). The Ceratolithus acutus first appearance datum is not present at Site 237, but is apparent at the other three sites. It has an age of 4.9 m.y. (Ryan, et al., 1974). The last appearance of Discoaster quinqueramus has an age of 5.6 m.y. (Ryan, et al., 1974) and is present at all four sites.

In addition to these three datums a fourth time-line is drawn at 6.6 m.y. on Figure 2. At Site 360 this datum is defined by the first appearance of Amaurolithus primus at 6.6 m.y. (Bukry, 1973 and 1975). At the other three sites it has been inferred, assuming constant sedimentation rates between the closest known datums and is consistent with known biostratigraphy and sedimentation rates. The base of the Messinian stage is at approximately 6.6 m.y. (Ryan, et al., 1974).

PRESENTATION OF DATA

Introduction

Biostratigraphy, lithology, sample spacing and ages for all four sites are shown in Figure 2. All other data referred to below are shown in Figures 3, 4, 5 and 6 for Sites 231, 237, 249, and 360 respectively. Running averages (over three adjacent points) have been computed for all data plotted in Figures 3, 4, 5 and 6 (except % Quartz and %Pyrite in Figure 3) and are superimposed on the raw data.

All data are plotted versus a linear time scale, which has been defined by the four faunal datums discussed above. Spacing between data points has been expanded or contracted as needed to make the data fit the linear time scale. The core numbers are shown in each figure for convenience.

Site 231

No oxygen isotope analyses were done on samples from Site 231 because the forams are poorly preserved.

Calcium Carbonate Analyses: The % $CaCO_3$ in samples from Site 231 oscillates between highs reaching 60% $CaCO_3$ and lows of 40% $CaCO_3$. The two low intervals were at about 6.6 m.y. to 6.0 m.y. (earliest Messinian) and about 4.5 to 4.2 m.y. (Early Pliocene). There is a steady decline in the %$CaCO_3$ from the peak at about 5.5 m.y., across the Miocene-Pliocene boundary, and into the Early

Figure 3: Per cent $CaCO_3$, grain size data, and quartz and pyrite content of samples from Site 231 in the Gulf of Aden. Vertical scale has been adjusted to the linear age scale discussed in the text. Datums are the same as those in Figure 2. Light lines represent the raw data, while the heavy lines represent three point running averages. Core numbers are given at the left for reference.

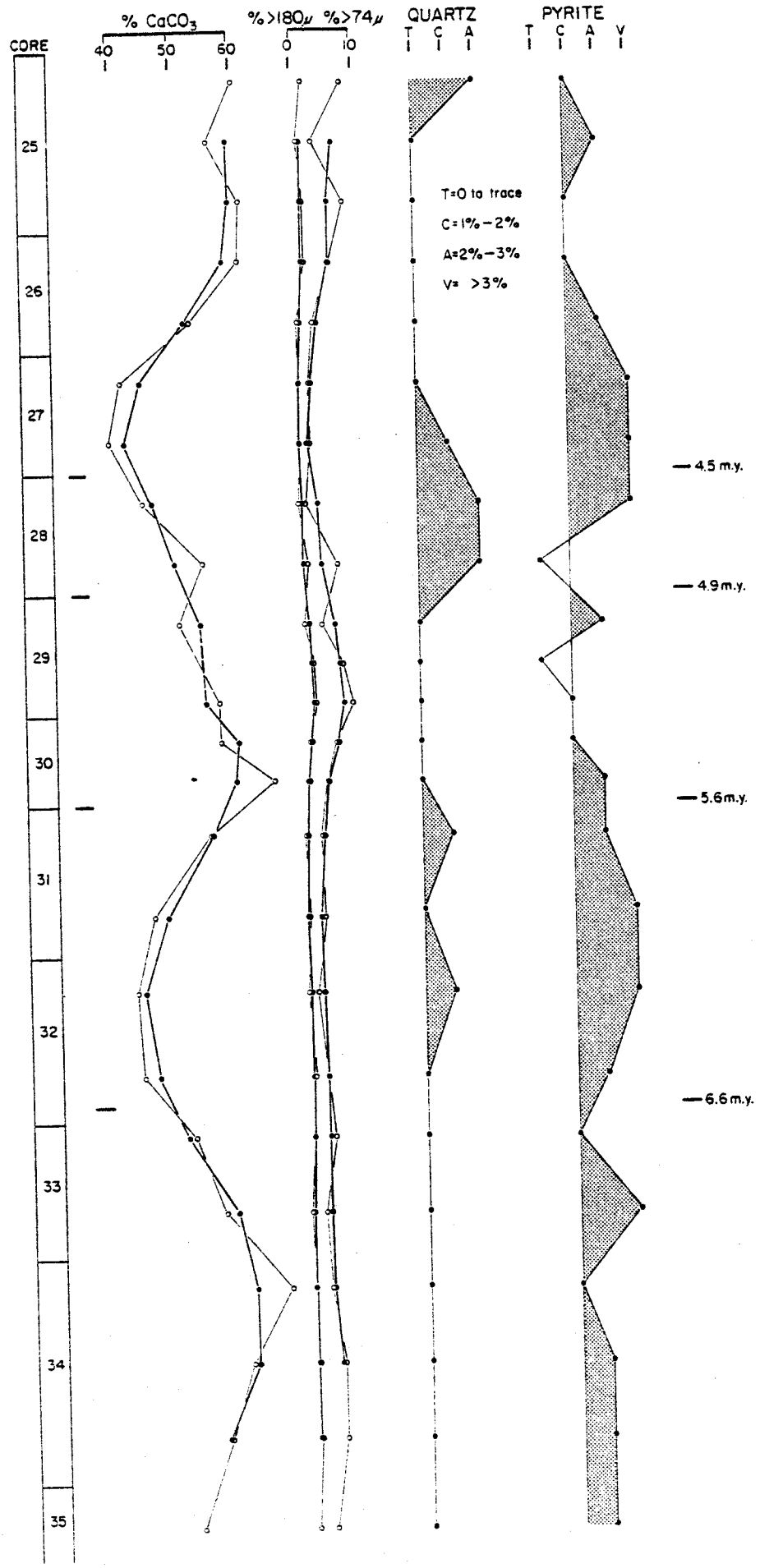
CORE
% CaCO3
40
50
60
%>180μ
%>74μ
0
10
QUARTZ
T C A
PYRITE
T C A V
T=0 to trace
C=1%–2%
A=2%–3%
V= >3%
25
26
27
28
29
30
31
32
33
34
35
4.5 m.y.
4.9 m.y.
5.6 m.y.
6.6 m.y.

Pliocene to about 4.5 m.y.

Size Fractions: The weight per cent >180μ plot runs parallel to the weight per cent >74μ plot, but changes are less pronounced in the >180μ plot than in the >74μ plot. The per cent >74μ is low (<10%) for all samples.

There is a rough correlation between the two periods of low per cent $CaCO_3$ and periods with low per cent >74μ. Since most of the sand sized particles are forams, low per cent $CaCO_3$ in conjunction with low per cent >74μ are thought to indicate periods of low foram productivity.

Quartz and Pyrite: The periods of low foram productivity mentioned above correspond roughly to periods of high detrital quartz input and high pyrite formation in the >74μ <180μ size fraction. These can be interpreted as periods of low sea level (increased detrital quartz input) and stagnation (drop in foram productivity and increase in pyrite formation).

In addition to quartz and pyrite the sediments at Site 231 contain minor amounts (generally <1% of feldspar, mica, volcanic glass and heavy minerals. Minor amounts of authigenic dolomite and zeolite are also present throughout the sampled sections.

Site 237

Oxygen Isotope Analyses: The running average of the oxygen isotope data varies between -0.25 per mil and -0.75

Figure 4: Oxygen isotope analyses, per cent fragments, per cent $CaCO_3$ and grain size data for Site 237 on the Mascarene Plateau in the western Indian Ocean. Symbols and scales are the same as in Figure 3.

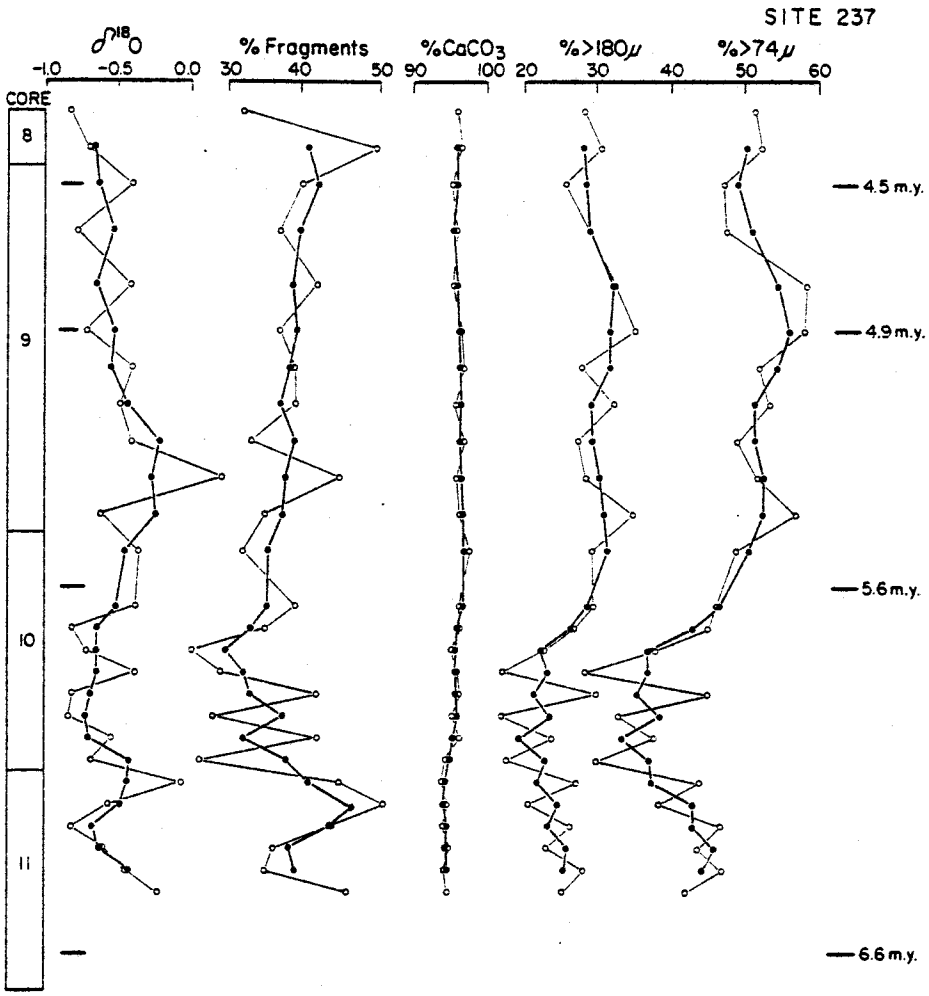
SITE 237
$\delta^{18}O$
-1.0 -0.5 0.0
% Fragments
30 40 50
%CaCO3
90 100
%>180μ
20 30 40
%>74μ
50 60
CORE
8
9
10
11
4.5 m.y.
4.9 m.y.
5.6 m.y.
6.6 m.y.

per mil. There is a short fluctuation toward more positive values at about 6.2 m.y. to 6.5 m.y., followed by an abrupt decline. Then, from 6.0 m.y. to 5.2 m.y. the $\partial^{18}O$ values increase steadily from -0.75 per mil to -0.25 per mil. From 5.2 m.y. onward into the early Pliocene, the $\partial^{18}O$ values decrease gradually.

Per cent Fragments: No significant events are discernable in the percentage of fragments in the >74μ <180μ size fractions from Site 237. The $\partial^{18}O$ values were plotted against the percentages of fragments for the same samples. The result is shown in Figure 7A. There is no correlation (coefficient of determination = 0.07).

Calcium Carbonate Analyses: The per cent calcium carbonate is consistently between 94% and 97%. Before ~5.7 m.y. all values are <95%, while after that time all values are >95%.

Size Fractions: The weight per cent of material >180μ at Site 237 changes in parallel with the weight per cent >74μ. From approximately 6.3 m.y. to approximately 5.9 m.y. there is a slight decrease in the amount of sand sized material, then an increase in the sand fraction begins and continues until approximately the Miocene-Pliocene boundary (5.2 m.y.). The large size fractions continue at a fairly constant percentage during the early Pliocene.

Since nearly all of the particles >74μ are planktonic

forams these changes in the percentage of coarse fractions can be interpreted in terms of productivity. Foram productivity was at a low at about 5.9 m.y., then, from 5.9 m.y. to 5.2 m.y. productivity increased. This increase in forams corresponds in time to the increase in $\%CaCO_3$, as might be expected.

It should be noted that the per cent >74μ at Site 237 is up to 10 times greater than the per cent >74μ at Site 231 in the Gulf of Aden.

Minerals: Microscopic examination of smear slides and size fraction separates revealed that <1% of the sediment at Site 237 is mineral grains. Trace amounts of quartz, pyrite and mica were observed.

Site 249

Oxygen Isotope Analyses: There is a pronounced decrease of nearly 0.75 per mil in the oxygen isotope values during the interval between 5.6 m.y. and 5.2 m.y. (end of the Messinian stage) at Site 249.

Per cent Fragments: The decrease in $\partial^{18}O$ values corresponds to a decrease in the percentage of fragments in the samples analysed for ^{18}O content. $\partial^{18}O$ (running average) is plotted versus the percentage of fragments (running average) in Figure 7B. The data show a good fit (coefficient of determination = 0.73) to the linear regression superimposed on the graph. This implies that the

Figure 5: Oxygen isotope analyses, per cent fragments, per cent $CaCO_3$ and grain size data for Site 249 on the Mozambique Ridge in the western Indian Ocean. Symbols and scales are the same as in Figure 3.

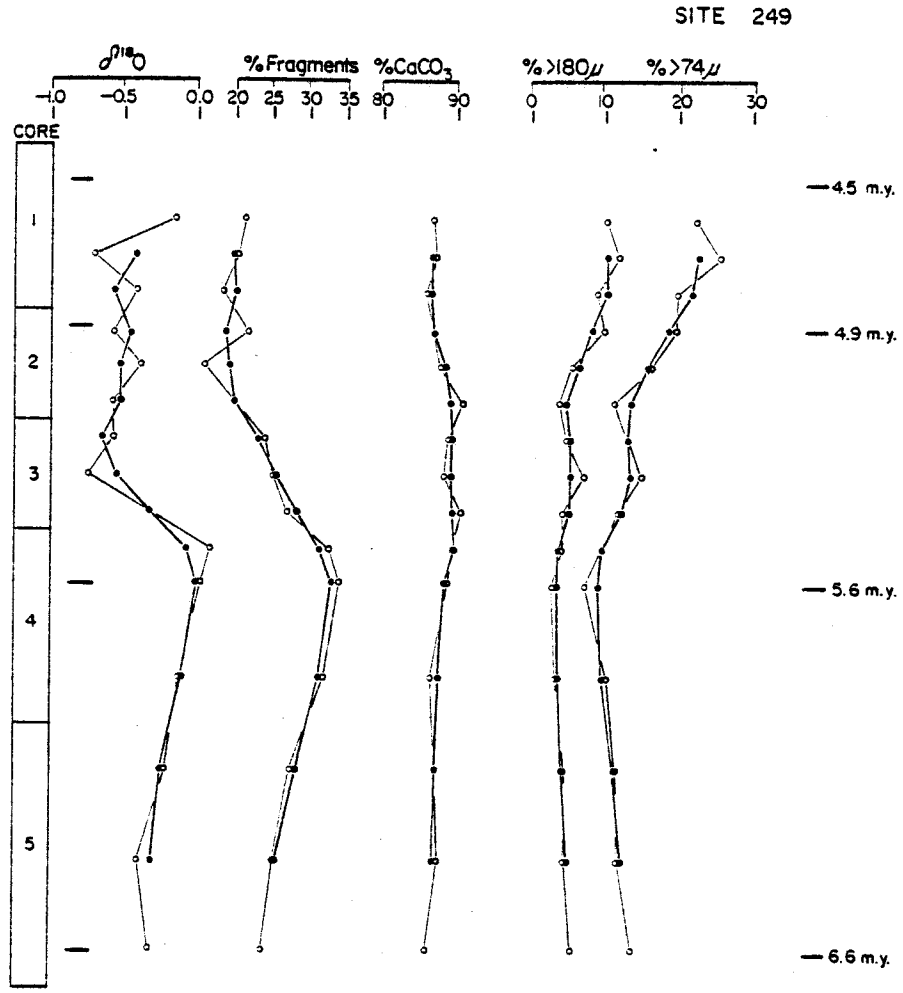
SITE 249
δ18O
−1.0
−0.5
0.0
% Fragments
20
25
30
35
% CaCO3
80
90
% >180μ
% >74μ
0
10
20
30
CORE
1
2
3
4
5
4.5 m.y.
4.9 m.y.
5.6 m.y.
6.6 m.y.

$\partial^{18}O$ values have been strongly biased by the fragments contained in the samples and, while the drop in $\partial^{18}O$ may be real, it may be smaller than indicated in Figure 5.

Calcium Carbonate Analyses: The percentage of calcium carbonate in the sediment at Site 249 stays consistently between 86% and 91%, with the higher values between 5.6 m.y. and 5.2 m.y.

Size Fractions: When plotted against depth in core, the percentage of material >180μ runs parallel to the percentage of material >74μ. Beginning at about 5.6 m.y. there is a general increase in large grains through the Messinian and across the Miocene-Pliocene boundary (5.2 m.y.). Since the >74μ size fractions at this site are nearly 100% forams, this general increase in large grains indicates an increase in forams. This may be attributed to increasingly better preservation of the large forams as dissolution decreased (see Per cent Fragments above) during this time period.

Minerals: Microscopic studies of smear slides and coarse size fractions showed <1% mineral grains throughout the sampled cores. Trace amounts of quartz, pyrite and mica were observed.

Site 360

Oxygen Isotope Analyses: Oxygen isotope values for

Figure 6: Oxygen isotope analyses, per cent fragments, per cent $CaCO_3$ and grain size data for Site 360 on the upper continental rise off South Africa. Symbols and scales are the same as in Figure 3.

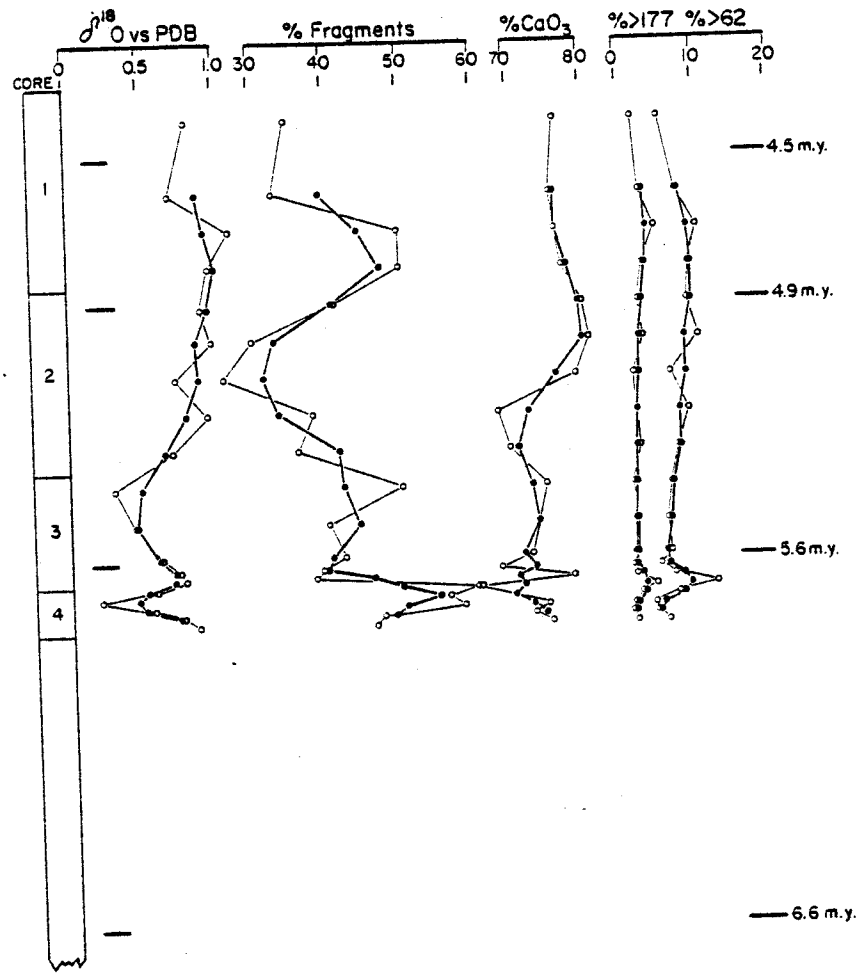
δ18O vs PDB
0
0.5
1.0
% Fragments
30
40
50
60
%CaO3
70
80
%>177 %>62
0
10
20
CORE
1
2
3
4
4.5 m.y.
4.9 m.y.
5.6 m.y.
6.6 m.y.

the latest Miocene at Site 360 fluctuate between 0.25 per mil and 0.75 per mil with lows at about 5.7 m.y. and 5.4 m.y. Oxygen isotope values decrease between 5.6 m.y. and 5.3 m.y., then begin an increase which continues until about 4.8 m.y. The $\partial^{18}O$ values in the early Pliocene stay between about 0.75 per mil and 1.00 per mil.

Per cent Fragments: At Site 360 there is a general decrease in the amount of fragmentation of the >74μ <180μ size fraction between 5.5 m.y. and 5.0 m.y. There is no apparent relationship between the percentage of fragments in the samples and the $\partial^{18}O$ values obtained for those samples (see Figure 7C). The coefficient of determination for the closest-fitting linear regression for these two data sets is 0.24.

Calcium Carbonate Analyses: The running average for the $\%CaCO_3$ data remains consistently between 70% and 75% until about 5.2 m.y. when it increases to 75% to 80%.

Size Fractions: Sand sized particles (i.e. forams) are not abundant at Site 360, the per cent of material >62μ being generally less than 10%. There is a slight increase in the coarse fraction beginning at about 5.6 m.y. and continuing to about 4.8 m.y.

Minerals: Examination of smear slides and coarse size fractions revealed that the sediments at Site 360 are composed of less than 1% mineral grains. Trace amounts of quartz, pyrite and mica were identified.

Figure 7: Running averages of the oxygen isotope data from each site plotted against the percentage of fragments (running averages) in the samples analysed. The coefficients of determination indicate the quality of the fit to the linear regression shown in each figure. Values close to 1.00 indicate a better fit than values close to 0.00.

A: Site 237 - no correlation

B: Site 249 - moderate to strong correlation

C: Site 360 - little or no correlation

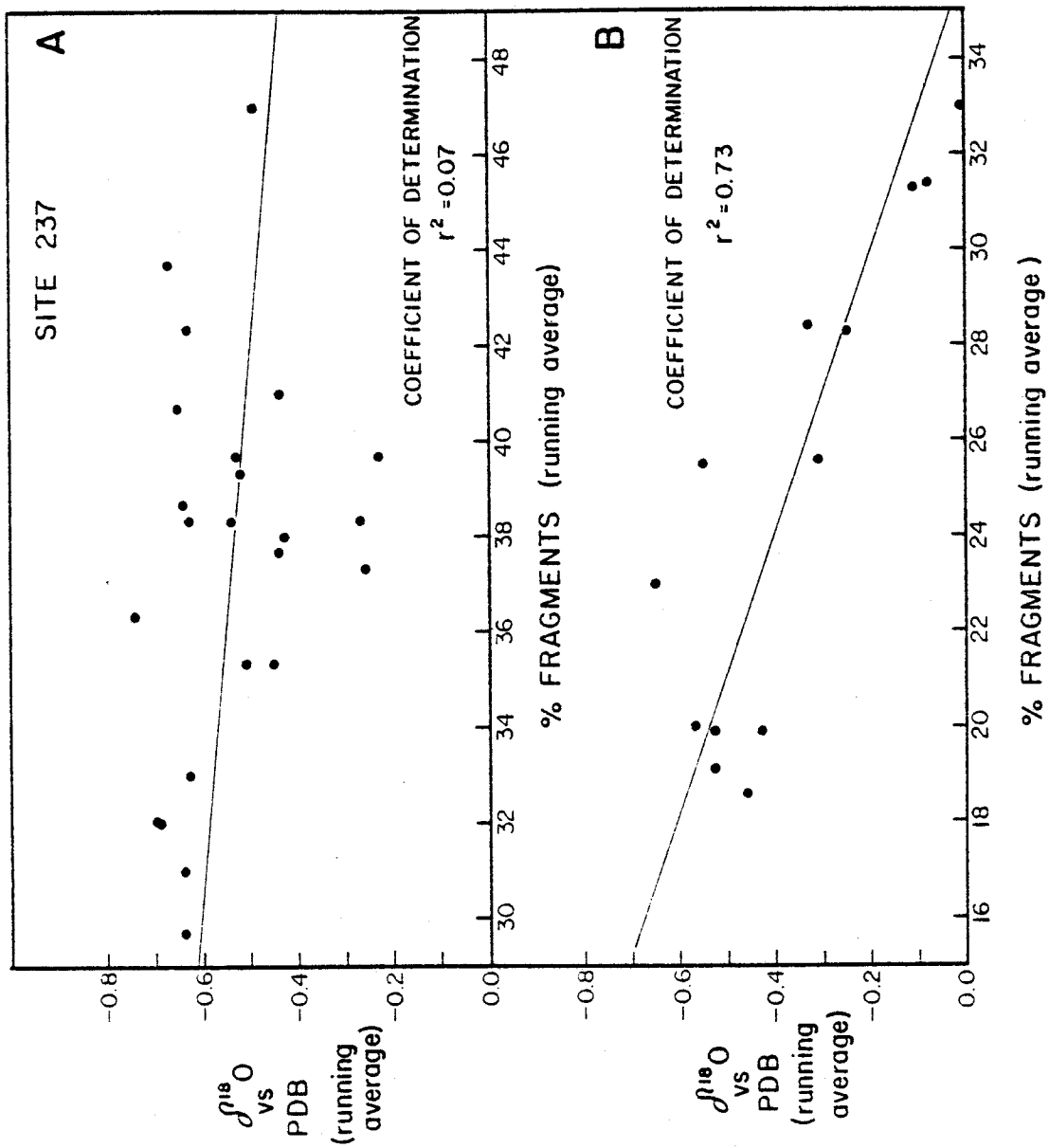
A
SITE 237
COEFFICIENT OF DETERMINATION
r^2 = 0.07
% FRAGMENTS (running average)
$\delta^{18}O$ vs PDB (running average)
B
COEFFICIENT OF DETERMINATION
r^2 = 0.73
% FRAGMENTS (running average)
$\delta^{18}O$ vs PDB (running average)

SITE 360

C

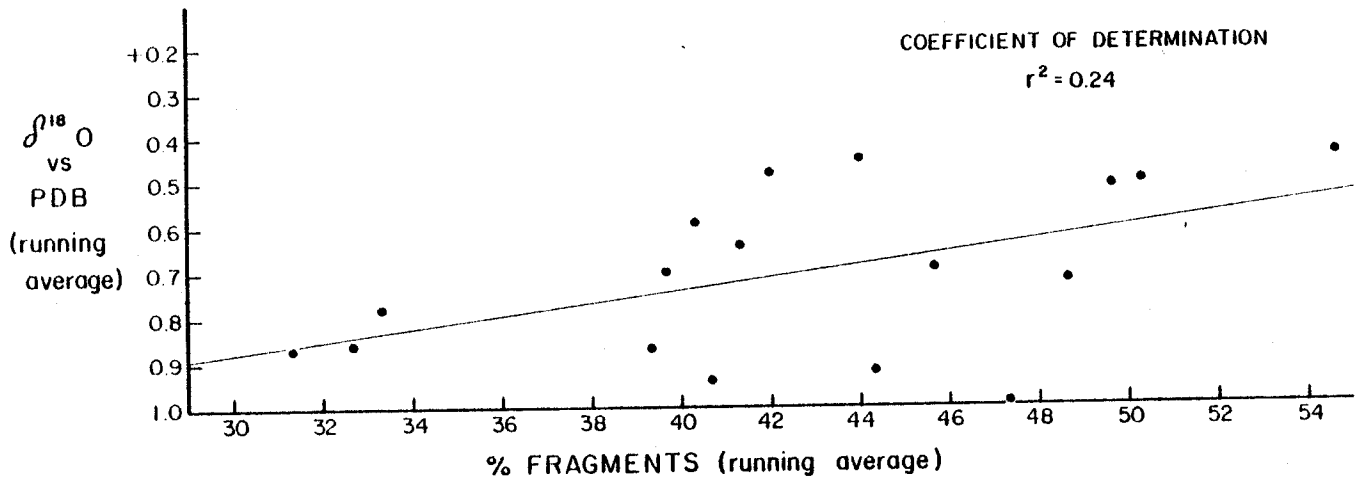
COEFFICIENT OF DETERMINATION
$r^2 = 0.24$
$\delta^{18}O$ vs PDB (running average)
+0.2
0.3
0.4
0.5
0.6
0.7
0.8
0.9
1.0
30
32
34
36
38
40
42
44
46
48
50
52
54
% FRAGMENTS (running average)

Discussion

Figures 8, 9, 10 and 11 show the oxygen isotope, per cent fragments, per cent calcium carbonate and per cent >74μ data, respectively, for all sites. In each case the running average of the data set is plotted against the linear time scale previously discussed.

Of the three oxygen isotope plots only one (Site 237) shows an increase in ∂O^{18} values during the latest Miocene followed by a decrease which continues into the early Pliocene (see Figure 8). The other two sites (249 and 360) display low ∂O^{18} values in approximately the same time interval during which Site 237 shows higher values. Site 360 has the highest isotopic values of the three sites, followed by Site 249, and Site 237 has generally the lowest. This is consistent with the relative latitudes of the three sites (Figure 1). The colder high latitudes have high values while the warmer low latitudes have low values.

The percentage of fragments in the >74μ <180μ size fractions from the three sites varies genearally independently at each site, although Sites 249 and 360 both show decreasing fragmentation (i.e., dissolution) between 5.6 m.y. and 4.9 m.y.

The percent calcium carbonate in the bulk samples also varies independently at each site. Site 231 in the Gulf of Aden has the lowest per cent calcium carbonate. The three sites in the open ocean are ranked according to latitude: the highest latitude site (360) has the lowest

Figure 8: Oxygen isotope data plotted versus age for DSDP Sites 237, 249 and 360. Scales are the same as in Figure 3.

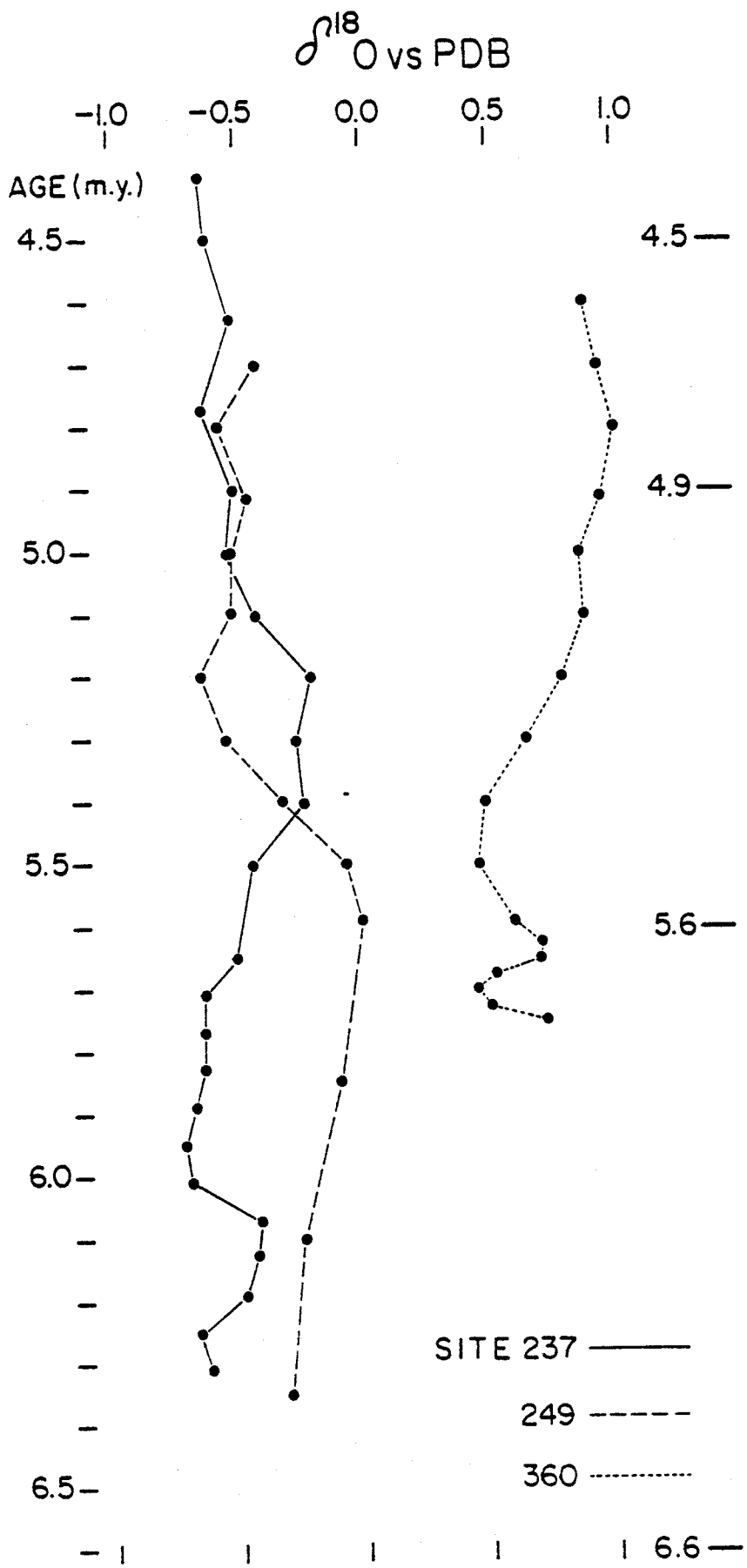
δ18O vs PDB
-1.0
-0.5
0.0
0.5
1.0
AGE (m.y.)
4.5
5.0
5.5
6.0
6.5
4.5
4.9
5.6
6.6
SITE 237
249
360

Figure 9: Percentage of fragments in the >74μ <180μ size fractions from DSDP Sites 237, 249 and 360 plotted versus age. Scales are the same as in Figure 3.

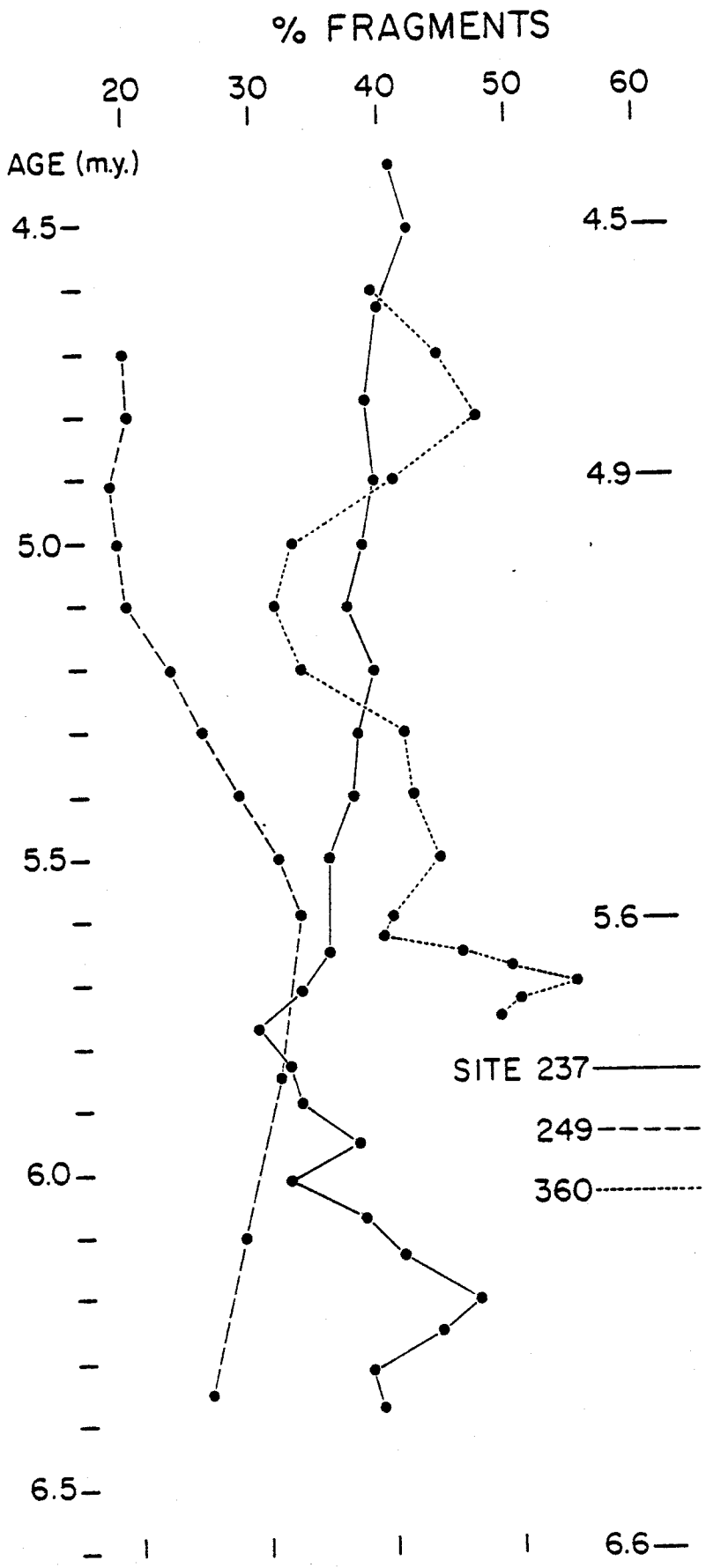
% FRAGMENTS
20
30
40
50
60
AGE (m.y.)
4.5
5.0
5.5
6.0
6.5
4.5
4.9
5.6
6.6
SITE 237
249
360

Figure 10: Per cent $CaCO_3$ in bulk samples from DSDP Sites 231, 237, 249 and 360 plotted versus age. Scales are the same as in Figure 3.

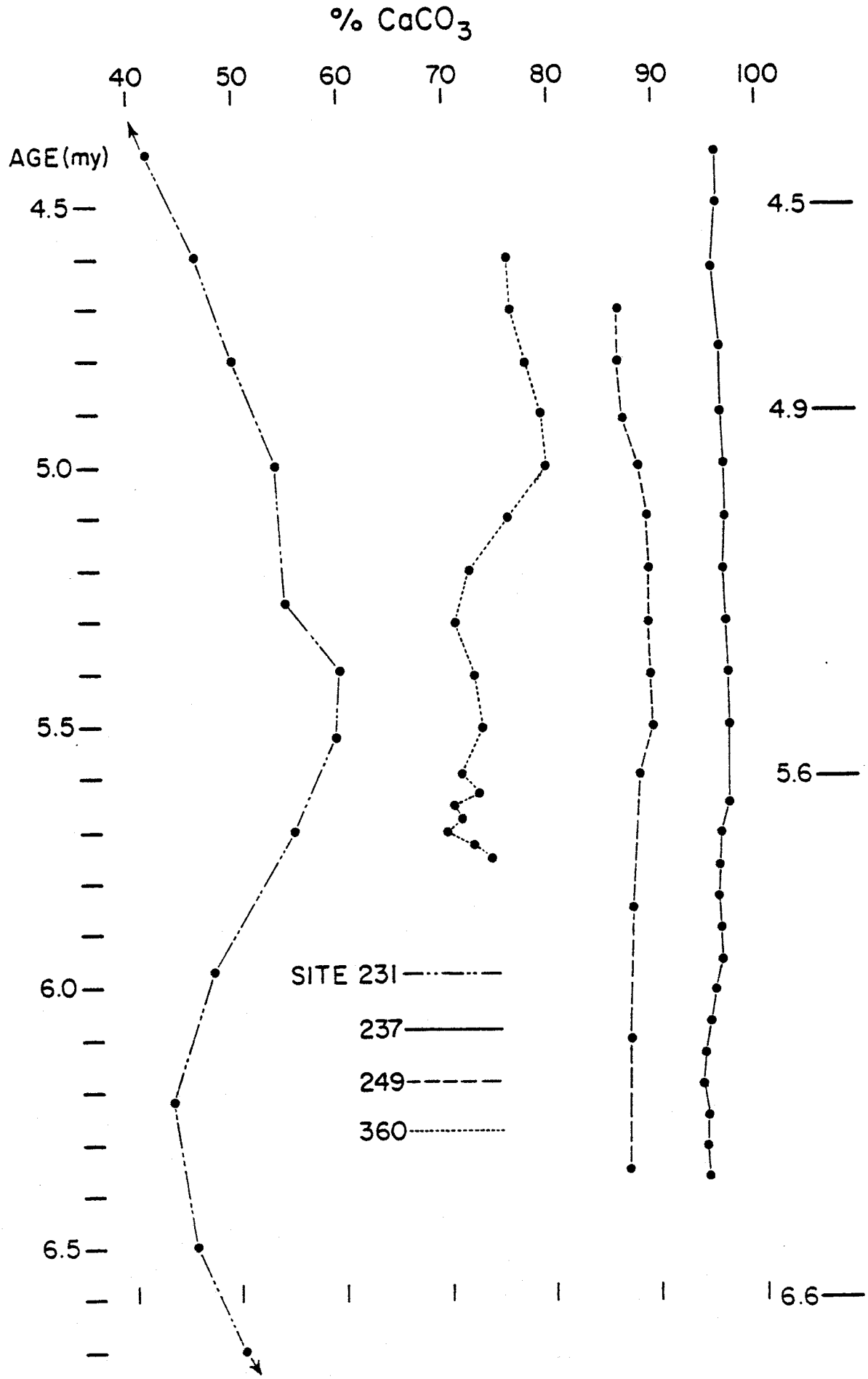
% CaCO3
40
50
60
70
80
90
100
AGE (my)
4.5
5.0
5.5
6.0
6.5
4.5
4.9
5.6
6.6
SITE 231
237
249
360

Figure 11: Per cent >74μ plotted versus age for DSDP Sites 231, 237, 249 and 360. Scales are the same as in Figure 3.

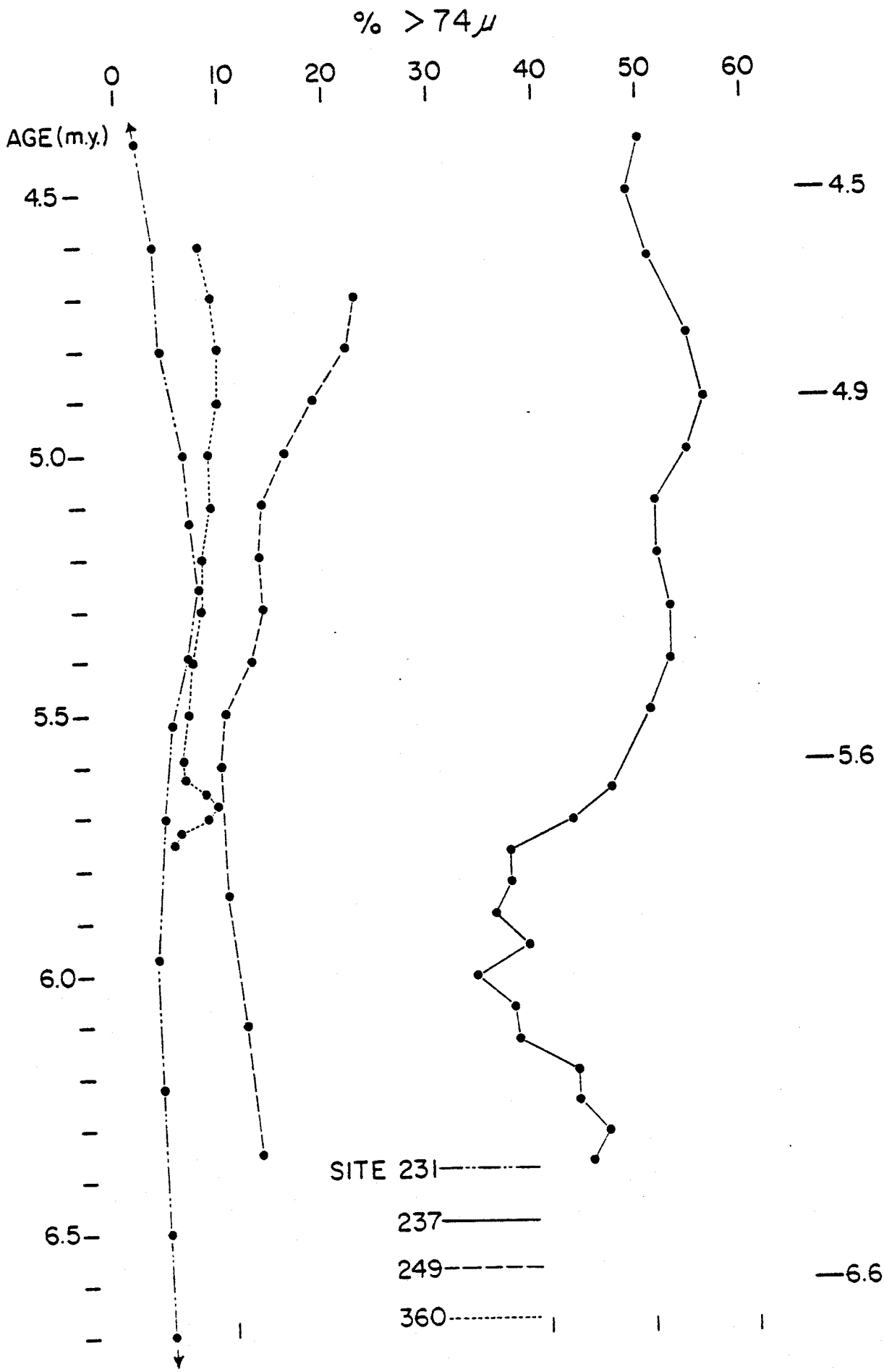
% >74μ
0
10
20
30
40
50
60
AGE (m.y.)
4.5
5.0
5.5
6.0
6.5
—4.5
—4.9
—5.6
—6.6
SITE 231
237
249
360

calcium carbonate content, while the lowest latitude site (237) has the highest calcium carbonate content (see Figure 10). Site 231 in the Gulf of Aden has the lowest calcium carbonate content because of its terrigeneous component.

The weight per cent >74μ plots for Sites 249 and 360 both show lows near 5.6 m.y. (Figure 11). Sites 237 and 231 also have low intervals, but they are about 0.4 m.y. earlier (at approximately 6.0 m.y.)

FACTORS AFFECTING DATA

The various types of data presented here can reflect one or more of many processes or conditions existing in the oceans either at the time of deposition or after. These processes and conditions are discussed below in the context of analyses done on sediments from DSDP Sites 231, 237, 249 and 360.

Oxygen Isotope Analyses

The $^{18}O/^{16}O$ ratio in a foraminiferal test is controlled by two factors: 1) the isotopic composition of the water from which the calcium carbonate was precipitated and, 2) the temperature at which precipitation took place (Urey, 1947 and Urey, et al., 1951). Surface waters, where the forams analysed here deposited their tests, change temperature with the seasons and with climatic fluctuations, such as glaciations. Bottom waters can be assumed to have maintained a constant temperature since the establishment of the Antarctic ice sheet in the mid-Miocene (Shackleton and Kennett, 1975b).

The isotopic composition of the world ocean fluctuates with the expansion and contraction of glacial ice (Emiliani, 1955). This is because the vapor pressure of H_2O^{16} is slightly greater than that of H_2O^{18}, causing water containing the lighter isotope to be preferentially evaporated, precipitated and hence incorporated into the ice sheets. A large volume of ice increases the $\delta^{18}O$ of the world ocean

and therefore also of the foram tests deposited in it. Cold temperatures increase the rate at which ^{18}O is incorporated into precipitating calcium carbonate. The two effects of temperature and isotopic composition of the ocean, then, add constructively, since cold temperatures and large ice volumes tend to occur together.

There are several factors in addition to glacial ice volume that can change the isotopic composition of ocean water, particularly of the surface water, locally. Proximity to a large source of fresh (isotopically light) water, restricted circulation and unbalanced evaporation/precipitation budget can all affect the $^{18}O/^{16}O$ ratio of ocean water locally. None of these factors are considered to be relevant to DSDP Sites 237, 249 or 360.

Per cent Fragments

The percentage of fragments of foraminifera relative to whole foraminifera in a sample is directly related to the intensity of post-depositional solution which was at work. The amount of dissolution, in turn, is related to many factors. The temperature of the water is inversely proportional to the amount of dissolution, but, since the bottom waters during the Late Miocene and early Pliocene can be assumed to have had a constant temperature (Shackleton and Kennett, 1975b) this is not a concern here. The amount of dissolved salts in the water also controls how much $CaCO_3$ can be dissolved. Since the Mediterranean

"salinity crisis" removed approximately 6 per cent of the salt from the World Ocean (Ryan, 1974) during the latest Miocene, dissolution of carbonate may increase throughout the oceans at this time. Periods of high dissolution (i.e., high percentage of fragments) have been correlated with interglacial periods (Hays, et al., 1969 and Thompson, 1976). It is thought that these periods of high dissolution may reflect the deposition of large volumes of calcium carbonate (i.e., the extraction of large amounts of $CaCO_3$ from the ocean water) in other parts of the ocean (Luz and Shackleton, 1975). An alternative explanation is that the destruction of terrestrial vegetation which would occur with the onset of a glacial period increases the amount of dissolved CO_2 in the ocean, causing an increase in $CaCO_3$ dissolution (Shackleton, 1976). This is consistent with the observation that episodes of intense dissolution reach their peaks about 5,000 years after the oxygen isotopically defined interglacial stages with which they are correlated reach their peaks (Shackleton and Opdyke, 1973).

Calcium Carbonate Analyses

The percentage of calcium carbonate in a bulk sediment sample is the result of the following three factors: 1) the rate of carbonate deposition, 2) the rate of deposition of non-carbonate components (e.g., terrigenous clastics and siliceous ooze) and 3) the amount of subsequent dissolution of the carbonates. The calcium

carbonate deposition rate is directly related to the productivity of calcareous fauna, mainly foraminifera. The factors controlling productivity are not well understood, but temperature and nutrient supply are probably the primary influences (Bé, et al., 1973). The rate of deposition of non-carbonate components is related to the productivity of siliceous fauna and is also affected by changes in the drainage patterns and humidity in nearby continental areas, as well as wind directions and sea level. None of the sites in this study contain a significant amount of siliceous ooze, and only Site 231 in the Gulf of Aden has a significant clastic component. The third factor, dissolution, is thought to have a greater affect than faunal productivity (Berger, 1973). Dissolution is discussed above under the heading "Per cent Fragments."

It is impossible, in the present study, to separate the effects of faunal productivities, rates of deposition of various components, and changes in intensity of dissolution. It has been shown, however, in Pleistocene deep sea sediments that relative carbonate-rich and carbonate-poor intervals correspond to glacial and interglacial periods respectively (Arrhenius, 1952; Thompson and Saito, 1974 and Thompson, 1976). The calcium carbonate analyses presented here are interpreted in light of this well-established, general correlation.

Per cent Coarse Fraction

There are four major factors that can determine the percentage of coarse (>74μ) material in sediment. They are:

1) Currents can sort grains and concentrate a particular size in one place. This is not considered to be a factor at DSDP Sites 231, 237, 249 or 360 since none showed signs of currents, erosion or reworking.

2) Changes in the quantity of terrigenous sediment input (as a result of changes in humidity, atmospheric circulation, drainage patterns or sea level) can affect the size distribution. The samples from DSDP Sites 237, 249 and 360 examined in this study have negligible terrigenous components. DSDP Site 231 (in the Gulf of Aden), however, contains significant quantities of terrigenous material and may reflect changes in climate in nearby Somalia.

3) The relative productivity of large foraminifera versus small forams and nannofossils directly affects the percentage of coarse grains in a sample. Bé, et al. (1973) has shown that the average size of G. orbulina changes with latitude and is probably related to nutrient supplies. Faunal productivity and size in the deep sea is not yet well understood.

4) Dissolution breaks down large tests (which make up nearly 100 per cent of the coarse fractions studied here) and creates smaller-sized fragments, thus reducing the percentage of coarse material. Alternatively, small, delicate forams may be preferentially dissolved, effectively

increasing the large-sized fractions. The varying percentages of fragments found in samples from DSDP Sites 237, 249 and 360 indicate that dissolution has had an effect on the coarse size fractions.

INTERPRETATION OF DATA

Thompson (1976), in a study of Pleistocene sediments from the Pacific Ocean, showed that periods of high dissolution (i.e., high percentage of fragmented forams), low percentage of calcium carbonate and low percentage of coarse grains correspond to periods of low $\partial^{18}O$ (i.e., interglacial periods) while periods of low dissolution, high percentage of calcium carbonate and high percentage of coarse grains correspond to periods of high $\partial^{18}O$ (i.e., glacial periods). The data from DSDP Sites 231, 237, 249 and 360 are interpreted on this basis.

At Site 231, alternating episodes of high and low dissolution are observed (see Figure 3). The low dissolution intervals are characterized by high percentage of calcium carbonate, high percentage >74μ, and low relative abundance of quartz. These episodes of low dissolution peak at approximately 7.3 m.y., 5.3 m.y. and 3.6 m.y. and are interpreted as episodes of cooler (glacial?) climate.

At Site 237 an increase in $\partial^{18}O$ begins at about 5.7 m.y. (see Figure 4) and reaches a peak at about 5.3 m.y. This is interpreted as a cooling event and should be accompanied by a low in dissolution. The percentage of fragments does not indicate a low in dissolution, but the coarse fraction does increase sharply and the percentage of calcium carbonate does exhibit slightly (1% to 2%) higher values during the period from 5.7 m.y. to 4.9 m.y.

A cool period with a peak at about 5.3 m.y. at this site is thought to correspond to a period of low dissolution (peak at about 5.3 m.y.) at Site 231.

The data from Site 249 is not easily interpreted. After 5.6 m.y. there is a steady decrease in the percentage of fragments, a steady increase in the percentage >74μ, and an increase in the percentage of calcium carbonate (see Figure 5), all of which indicate decreasing dissolution which is usually associated with cooling climate. The oxygen isotope values, however, drop after 5.6 m.y., suggesting a warming trend. The percentage of fragments data and the oxygen isotope data show a high degree of correlation (see Figure 7B), suggesting that the isotope analyses have been biased by the foram fragments in the samples. The oxygen isotope data from this site should be used with caution, the other types of data being given greater weight. On the basis of the percentage of fragments, a cool period is tentatively suggested to have its peak at about 5.0 m.y. (see Figure 5).

At Site 360, the percentage of fragments, the percentage of calcium carbonate, and the percentage of material >62μ (see Figure 6) all indicate a period of low dissolution with a peak at about 5.0 m.y. Although this would imply a cool climate, no corresponding event is seen in the oxygen isotope data. There is no apparent explanation for this lack of an isotopic event.

Cores from each site contain some evidence for a

cool episode near the Miocene/Pliocene boundary (approximately 5.2 m.y. (Ryan, et al., 1974). The peak of this cool period is at about 5.0 m.y. at Sites 249 and 360 and at about 5.3 m.y. at Sites 231 and 237, according to the linear time scale set up on the basis of faunal datums.

CONCLUSIONS

1. A period of cool climate (expansion of Antarctic glaciation) is proposed for the period between about 5.7 m.y. and 4.9 m.y. with the culmination at about 5.0 m.y. to 5.3 m.y. This event may correspond to the late Miocene glacial expansion reported by Shackleton and Kennett (1975a and 1975b).

2. The cool period is not obvious in the oxygen isotope data from Sites 249 and 360, implying that there are too many factors influencing the oxygen isotope composition of bulk planktonic foram samples for them to be universally useful for the detection of an isotopic event as small as the late Miocene event. This also casts doubt on the usefulness of the late Miocene event as a world-wide stratigraphic marker.

3. Some of the data is not consistent with predicted trends. Local and regional conditions, such as temperature, nutrient supply and foram productivity are therefore suggested to be of greater importance than world-wide events in the sedimentation history of these sites.

4. The biostratigraphy currently available in the Initial Reports of the Deep Sea Drilling Project for the late Miocene and early Pliocene is not sufficiently precise to correlate an event more closely than about 0.3 m.y.

5. Because of the limitations of the biostratigraphy, and because a convincing correlation of oxygen isotopic

events could not be made, no significant conclusions can be drawn regarding the relative timing of events within and outside of the Mediterranean during the Messinian "salinity crisis."

APPENDIX A

Checks on size separation techniques.

As a check on the efficiency of the wet sieving technique, all of the samples from Site 231 were dry sieved using both a 180μ and a 74μ sieve after they had been wet sieved with the 74μ sieve. The small amount of material that passed through the 74μ sieve was collected and weighed. This weight was then subtracted from the weight of each >74μ sample as determined by wet sieving. Each >74μ sample weight was lowered by less than 1%, which is a per cent change of between 6.38% and 13.13% (average = 9.42%). See Table II.

The per cent change, being nearly constant for all samples, does not change the relative %>74μ weights significantly, but merely shifts the entire %>74μ vs. depth curve slightly to the left (Figure 12).

All of the whole samples were air dried at room temperature and weighed before the 74μ wet sieving was performed. To check whether or not the air-drying technique was sufficiently efficient, one sample was weighed after air-drying, weighed again after 20 hours in a dessication jar, and weighed a third time after baking for 20 hours then cooling for 4 hours in a dessication jar. The results are shown in Table III. The weight after baking was less than 2% less than the air dried weight.

The sample chosen for this test had a lower $\%CaCO_3$

TABLE II

Site 231 %>74μ

sample	difference (wet sieve minus wet sieve and dry sieve)	% change
25-1	0.641	7.26
25-3	0.319	8.55
25-6	0.967	10.45
26-3	0.628	9.77
26-5	0.288	8.51
27-2	0.262	10.15
27-5	0.263	10.07
28-1	0.198	11.59
28-4	0.484	6.77
29-1	0.267	6.38
29-3	0.576	7.29
29-6	0.958	9.81
30-3	0.723	11.11
30-5	0.372	7.83
31-2	0.415	11.54
31-5	0.550	13.13
32-1	0.298	11.60
32-4	0.337	8.31
33-1	0.652	12.06
33-3	0.315	9.38
34-1	0.329	7.99
34-4	0.504	8.07
34-6A	0.589	9.16

Figure 12: Weight per cent >74μ at Site 231. Dark line with solid circles represents weight per cent >74μ after wet sieving. Light line with open circles represents weight per cent >74μ after additional dry sieving.

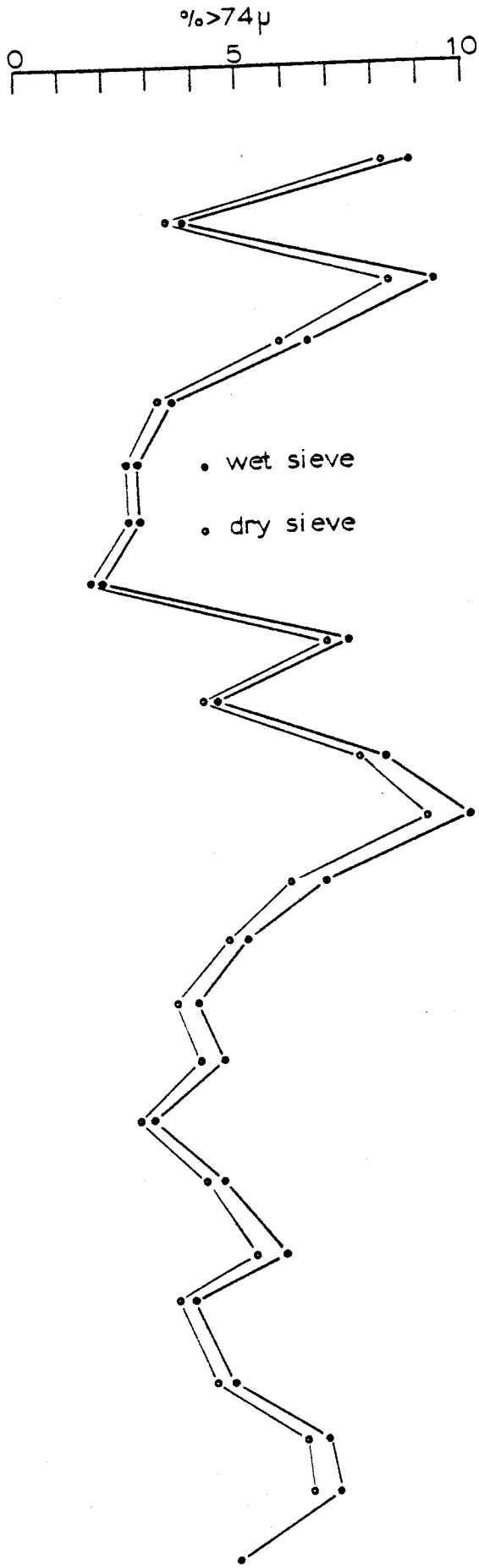
%>74μ
0
5
10
wet sieve
dry sieve

TABLE III

1.	air dried	10.00350 grams
2.	after 20 hours in dessicator	9.90960 grams
3.	after 20 hours in oven and 4 in dessicator	9.80385 grams

The per cent change from 1 to 3 = 1.9958%.

and a higher clay content than any of the other samples. Because of this, it can be assumed that the other samples would not have shown a greater weight loss had they been baked.

APPENDIX B

Data Tables

TABLE IV

Site 231

Core-section	Depth below top of section (cm)	% Quartz	% Pyrite	% $CaCO_3$	%>180μ	%>74μ
25-1	45	A	C	60.28	1.816	8.830
25-3	142	T	A	56.09	0.759	3.732
25-6	102	T	C	61.24	1.619	9.253
26-3	54	T	C	60.83	1.786	6.430
26-5	137	T	A	52.70	0.676	3.384
27-2	100	T	V	41.30	0.700	2.582
27-5	52	C	V	39.26	0.678	2.612
28-1	137	A	V	44.64	0.344	1.708
28-4	102	A	T	54.36	1.840	7.147
29-1	46	T	A	50.26	1.051	4.183
29-3	134	T	T	-----	2.462	7.900
29-6	95	T	C	56.67	2.819	9.764
30-3	52	T	C	57.05	1.695	6.507
30-5	143	T	A	65.57	1.439	4.754
31-2	100	C	A	55.10	0.607	3.598
31-5	43	T	V	45.28	0.947	4.189
32-1	143	C	V	42.57	0.704	2.570
32-4	101	T	A	43.39	1.643	4.056
33-1	148	T	C	51.69	1.242	5.408
33-3	143	T	V	56.51	0.729	3.357
34-1	101	T	C	67.19	0.984	4.116
34-4	50	T	A	60.62	1.461	6.242
34-6A	105	T	A	56.82	1.615	6.429
34-6B	140	---	---	33.25	-----	-----
35-3	99	T	A	51.92	1.025	4.129

TABLE V

Site 237

Core-section	Depth below top of section (cm)	$\partial^{18}O$	% Fractured >74μ <180μ fraction	% $CaCO_3$	% >180μ	% >74μ
8-5	140	-0.83	32	95.83	28.140	51.26
8-6	95	-0.70	50	96.54	30.372	52.24
9-1A	53	-0.41	40	95.15	25.637	47.02
9-1B	140	-0.77	37	95.92	28.937	47.40
9-2	101	-0.42	42	95.43	32.170	58.26
9-3A	51	-0.72	37	96.43	34.991	57.88
9-3B	140	-0.41	39	96.77	27.788	51.97
9-4	101	-0.49	39	95.88	32.112	53.32
9-5A	52	-0.42	33	96.94	27.350	48.89
9-5B	140	0.21	45	95.92	28.357	51.65
9-6	104	-0.61	35	96.43	34.890	56.82
10-1A	52	-0.36	32	97.67	29.269	48.74
10-1B	140	-0.38	39	96.34	29.525	46.00
10-2	101	-0.80	35	96.30	26.995	45.01
10-3A	51	-0.72	25	95.26	22.786	37.69
10-3B	140	-0.39	29	95.78	17.213	28.03
10-4	100	-0.82	42	96.34	29.943	44.90
10-5A	53	-0.85	28	95.36	17.014	32.87
10-5B	140	-0.55	42	96.33	23.829	37.57
10-6	104	-0.68	26	94.55	17.748	29.88
11-1A	45	-0.07	45	94.00	27.218	43.82
11-1B	140	-0.57	51	94.64	20.562	38.51
11-2	100	-0.82	44	94.20	26.355	46.83
11-3A	51	-0.62	36	94.92	23.100	43.74
11-3B	140	-0.45	35	94.33	28.093	46.92
11-4	100	-0.23	46	94.74	25.262	42.13

TABLE VI

Site 249

Core-section	Depth below top of section (cm)	$\partial^{18}O$	% Fractured >74 <180μ fraction	$\%CaCO_3$	% >180μ	% >74μ
1-2	74	-0.16	21.2	86.92	10.069	22.48
1-4	24	-0.71	20.2	87.18	11.942	25.60
1-5	97	-0.42	18.2	85.77	9.021	19.97
2-1	106	-0.57	21.7	86.86	9.996	19.75
2-3	52	-0.39	15.9	87.72	5.671	16.36
2-4	124	-0.63	19.7	90.88	4.013	11.30
3-2	24	-0.57	24.0	88.97	4.944	13.29
3-3	124	-0.74	25.3	88.39	7.296	15.15
3-5	82	-0.33	27.1	90.63	4.376	12.05
4-2	52	0.08	32.8	89.55	4.117	9.68
4-4	24	0.02	34.2	88.89	3.023	7.45
4-5	98	-0.12	32.1	86.64	3.586	10.50
5-1	124	-0.22	27.5	87.34	4.551	11.35
5-3	68	-0.40	25.4	87.70	4.921	11.98
5-5	24	-0.32	24.0	86.13	5.881	14.12

TABLE VII

Site 360

Core-section	Depth below top of section (cm)	$\partial^{18}O$	% Fractured (62-180μ fraction)	% $CaCO_3$	% >177μ	/ % >62μ
1-1	97	0.82	35.2	76.30	1.914	5.43
1-2	125	0.70	33.2	75.58	2.707	7.77
1-4	1	1.10	49.8	76.06	4.710	10.38
1-5	25	0.96	50.3	77.02	3.208	9.25
2-1	54	0.90	41.7	79.74	2.384	8.95
2-2	75	0.97	30.0	80.57	2.955	10.34
2-3	94	0.72	25.7	78.64	1.568	6.63
2-4	125	0.93	37.9	68.11	1.998	9.03
2-6	4	0.69	35.8	69.66	2.308	7.46
3-1	144	0.30	49.6	74.47	1.415	6.53
3-2	74	0.44	39.7	73.25	1.679	5.90
3-3	100	0.61	41.7	72.40	1.603	6.22
3-4	125	0.73	38.9	68.12	1.333	4.78
3-6	4	0.76	38.3	77.89	1.469	6.70
4-1	142	0.57	60.4	65.51	4.114	12.33
4-2	75	0.20	50.8	69.94	2.408	7.36
4-3	102	0.56	52.8	74.45	1.393	4.01
4-4	125	0.75	47.1	72.63	0.948	4.25
4-5	0-140	0.85	45.7	74.94	1.544	5.62

REFERENCES

Adams, C.G.; Benson, R.H.; Kidd, R.B.; Ryan, W.B.F.; Wright, R.C., 1977. The Messinian salinity crisis and evidence of Late Miocene eustatic changes in the world ocean, Nature, v. 269, p. 383-386.

Arrenhius, G., 1952. Sediment cores from the East Pacific, Swedish Deep-Sea Exped. (1947-1948) Reports, v. 5, nos. 1-4, p. 1-228.

Bé, A.W.H.; Harrison, S.M. and Lott, L., 1973. Orbulina universa d'Orbigny in the Indian Ocean. Micropaleontology, v. 19, no. 2, p. 150-192.

Berger, W.H., 1973. Deep-sea carbonates: Pleistocene dissolution cycles, Jour. Foram. Research, v. 3, p. 187-195.

Berggren, W.A., 1973. Biostratigraphy and biochronology of the late Miocene (Tort. & Mess.) of the Mediterranean in: Drooger, C.W. (ed.), Messinian Events in the Mediterranean Geodynamics Scientific Report No. 7 North-Holland Pub. Co., Amsterdam.

Blow, W.H., 1969. Late Middle Eocene to Recent planktonic foraminiferal biostratigraphy in: Brönnimann, P. and Renz, H.H. (eds.), Proceedings of the First International Conference on Planktonic Microfossils Geneva 1967, v. 1, p. 199-421, Leiden.

Bolli, H.M.; Ryan, W.B.F., et al., 1978. Initial Reports of the Deep Sea Drilling Project, Volume 40, Washington (U.S. Government Printing Office).

Bukry, D., 1973. Low-latitude coccolith biostratigraphic zonation; in: Edgar, N.T.; Saunders, J.B., et al., Initial Reports of the Deep Sea Drilling Project, Volume 15, p. 685-703.

_____, 1974. Coccolith zonation of cores from the western Indian Ocean and the Gulf of Aden, Deep Sea Drilling Project, Leg 24; in Fisher, R.L.; Bunce, E.T., et al., Initial Reports of the Deep Sea Drilling Project, Volume 24, Washington (U.S. Government Printing Office), p. 995-996.

_____, 1975. Silicoflagellate and coccolith stratigraphy, Deep Sea Drilling Project, Leg 29; in: Kennett, J.P.; Houtz, R.E.; et al., Initial Reports of the Deep Sea Drilling Project, Volume XXIX, Washington (U.S. Government Printing Office), p. 845-872.

Cita, M.B.; R.C. Wright; Ryan, W.B.F. and A. Longinelli, 1978. Messinian Paleoenvironments; in: Hsu, K., Montadert, L., et al., Initial Reports of the Deep Sea Drilling Project, Volume XLII, part 1, Washington (U.S. Government Printing Office).

Craig, H., 1957. Isotopic standards for carbon and oxygen and correction factors for mass spectrometric analysis of carbon dioxide, Geochim. Cosmochim. Acta, v. 12, p. 133-149.

Decima, F.P.; Medizza, F. and Todesco, L. 1978. Southeastern Atlantic Leg 40 Calcareous Nannofossils in: Bolli, H.M.; Ryan, W.B.F., et al., 1978 Initial Reports of the Deep Sea Drilling Project, Volume 40, Washington (U.S. Government Printing Office), p. 571-634.

Douglas, R.G. and Savin, S.M., 1973. Oxygen and carbon isotope analyses of Cretaceous and Tertiary foraminifera from the central North Pacific in: Initial Reports of the Deep Sea Drilling Project, Volume 17, p. 591-605, Winterer, E.L.; Ewing, J.I., et al., U.S. Government Printing Office.

_____, 1975. Oxygen and carbon isotope analyses of Tertiary and Cretaceous microfossils from Shatsky Rise and other sites in the North Pacific Ocean in: Larson, R.L., Moberly, R., et al., v. 32 of Initial Reports of Deep Sea Drilling Project, Washington (U.S. Government Printing Office).

Drooger, C.W., (ed.), 1973. Messinian Events in the Mediterranean Geodynamics Scientific Report No. 7, North-Holland Pub. Co., Amsterdam.

Emiliani, C., 1955. Pleistocene temperatures, Journal of Geology, v. 63, p. 538-578.

_____, 1966. Paleotemperature analysis of Caribbean cores P6304-8 and P6304-9 and a generalized temperature curve for the last 425,000 years, Journal of Geology, v. 74, p. 109-126.

_____, 1971. Depth habitats of growth stages of pelagic foraminifera, Science, v. 173, p. 1122-1124.

_____, 1977. Oxygen isotopic analysis of the size fraction between 62 and 250 micrometers in Caribbean cores P6304-8 and P6304-9, Science, v. 198, no. 4323, p. 1255-1256.

Fisher, R.L.; Bunce, E.T., et al., 1974. Initial Reports of the Deep Sea Drilling Project, Volume 24, Washington (U.S. Government Printing Office).

Folk, R.L., 1974. Petrology of Sedimentary Rocks, Hemphill Publishing Co., Austin, Texas.

Grazzini, C., 1977. Cenozoic paleotemperatures at Site 398, Northeastern Atlantic. Diagenetic effects on carbon and oxygen isotopic signal. preprint in: Initial Reports of the Deep Sea Drilling Project, Leg. 47B, Washington (U.S. Government Printing Office).

Harper, Howard and Barron, John, 1978. The Messinian event in the North Pacific Deep-Sea (Abs.), GSA Abstracts with Programs, v. 10, no. 7, Annual Meeting Toronto, p. 416.

Hayes, D.E.; Frakes, L.A., et al., 1975. Initial Reports of the Deep Sea Drilling Project, Volume 28, Washington (U.S. Government Printing Office).

Hays, J.D.; Saito, T.; Opdyke, N.D.; and Burckle, L.H., 1969. Pliocene-Pleistocene sediments of the equatorial Pacific: their paleomagnetic, biostratigraphic and climatic record, GSA Bull., v. 80, p. 1481-1514.

Hsu, K.J.; Montadert, L.; D. Bernoulli; M.B. Cita; A. Erickson; R.E. Garrison; R.B. Kidd; F. Mélierés; C. Müller, R. Wright, 1977. History of the Mediterranean salinity crisis, Nature, v. 267, p. 399-403.

Hülsemann, J., 1966. On the routine analysis of carbonates in unconsolidated sediments, Journal of Sed. Pet., June 1966, v. 36, p. 622-625.

Ingle, James C., Jr., 1978. Evidence of latest Miocene refrigeration and associated eustatic events in California and the North Pacific (Abs.), GSA Abstracts with Programs, v. 10, no. 7, Annual Meeting, Toronto, 1978, p. 427.

Jenkins, D.G., 1978. Neogene planktonic foraminifers from Deep Sea Drilling Project, Leg 40, Sites 360 and 362 in the southeastern Atlantic, in: Bolli, H.M.; Ryan, W.B.F., et al., 1978 Initial Reports of the Deep Sea Drilling Project, Volume 40, Washington (U.S. Government Printing Office).

Kennett, J.P., 1977. Cenozoic evolution of Antarctic glaciation, the circum-Antarctic Ocean and their impact on global paleoceanography, J. of Geophys. Res., v. 82, no. 27, p. 3843-3860.

_____, 1978. The development of planktonic biogeography in the southern ocean during the Cenozoic, Marine Micropaleontology, v. 3, p. 301-345.

Kennett, J.P.; N.J. Shackleton; S.V. Margolis; D.E. Goodney; W.C. Dudley and P.M. Kroopnick, 1979. Late Cenozoic oxygen and carbon isotopic history and volcanic ash stratigraphy: Deep Sea Drilling Project Site 284, South Pacific, Am. J. of Science, v. 279, p. 52-69.

Luz, B. and Shackleton, N.J., 1975. $CaCO_3$ solution in the tropical east Pacific during the past 130,000 years. Cushman Foundation for Foraminiferal Research Special Publication 13, p. 142-150.

Mayer, C., 1867. Cataloque systématique et descriptif des fossiles des terrains tertiaires qui se trouvent au musée fédéral de Zurich. Deuxiemè cahier: Mollusques, familles des Mactridés et des Pholadomyidés, Lib. Schabelitz.

Müller, C., 1974. Calcareous nannoplankton, Leg 25 (Western Indian Ocean) in: Simpson, E.S.W.; Schlick, R., et al., 1974 Initial Reports of the Deep Sea Drilling Project, Volume 25, Washington (U.S. Government Printing Office), p. 579-634.

Rio, D.; Mazzei, R. and Palmieri, G., 1976. The stratigraphic position of the Mediterranean upper Miocene evaporites, based on nannofossils, preprint submitted to La Ricerca Scientifica C.N.R., Roma, 1977.

Roth, P.H., 1974. Calcareous nannofossils from the North-Western Indian Ocean, Leg 24, Deep Sea Drilling Project in Fisher, R.L., et al., Initial Reports of the Deep Sea Drilling Project, Volume 24, p. 969-994.

Ryan, W.B.F., 1973. Messinian events in the Mediterranean in Drooger, C.W. (ed.), Konink. Ned. Akad. Wetensch, Amsterdam.

Ryan, W.B.F.; Cita, M.B.; Rawson, M. Dreyfus; Burckle, L.H. and Saito, T., 1974. A paleomagnetic assignment of Neogene stage boundaries and the development of isochronous datum planes between the Mediterranean, the Pacific and Indian Oceans in order to investigate the response of the World Ocean to the Mediterranean salinity crisis. Riv. Ital. Paleont. (Milano) v. 80, no. 4, p. 631-688.

Selli, R., 1960. Il Messiniano Mayer-Eymar 1867. Proposta di un neostratotipo, Giorn. di Geologia, Ann. Mus. Geol. Bologna ser. 2, 28, 1-30.

Shackleton, N.J., 1976. Carbon-13 in Uvigerina: Tropical rainforest history and the equatorial Pacific carbonate dissolution cycles (preprint). ONR Conference on the Fate of Fossil Fuel Carbonates, Jan. 1976, Honolulu, Hawaii.

Shackleton, N.J. and Kennett, J.P., 1975a. Paleotemperature history of the Cenozoic and the initiation of Antarctic glaciation: oxygen and carbon isotope analyses in Deep Sea Drilling Project sites 277, 279 and 281. in: Kennett, J.P., Houtz, K.E., et al., Initial Reports of the Deep Sea Drilling Project, Volume 29, p. 743-755, U.S. Government Printing Office.

_____, 1975b. Late Cenozoic oxygen and carbon isotopic changes at Deep Sea Drilling Project Site 284: implications for glacial history of the northern hemisphere and Antarctica in: Kennett, J.P., Houtz, K.E., et al., Initial Reports of the Deep Sea Drilling Project, Volume 29, p. 801-807, U.S. Government Printing Office.

Shackleton, N.J. and Opdyke, N.D., 1973. Oxygen isotope and paleomagnetic stratigraphy of equatorial Pacific core V28-238: oxygen isotope temperatures and ice volumes on a 10^5 and 10^6 year scale. Quaternary Research, v. 3, p. 39-55.

Simpson, E.S.W.; Schlich, R., et al., 1974. Initial Reports of the Deep Sea Drilling Project, Volume 25, Washington (U.S. Government Printing Office).

Thompson, P.R., 1976. Planktonic foraminiferal dissolution and the progress towards a Pleistocene equatorial Pacific transfer function, Journal of Foraminiferal Research, v. 6, no. 3, p. 208-227.

Thompson, P.R. and Saito, T., 1974. Pacific Pleistocene sediments: planktonic foraminifera dissolution cycles and geochronology, Geology, v. 2, no. 7, p. 333-335.

Urey, H.C., 1947. The thermodynamic properties of isotopic substances. J. Chem. Soc., v. 1947, p. 562-581.

Urey, H.C.; H.A. Lowenstam; S. Epstein and C.R. McKinney, 1951. Measurements of paleotemperatures and temperatures of the Upper Cretaceous of England, Denmark and the southeastern United States, GSA Bull., v. 62, p. 399.

Van Couvering, Judith A.H., 1978. Collapse of the Savanna-Mosaic Chronofauna in Holarctica: a "Messinian" terrestrial event (abs.) GSA Abstracts with Programs, v. 10, no. 7, Annual Meeting, Toronto, 1978, p. 508.

Vincent, E.; Frericks, W.E. and Heiman, M.E., 1974. Neogene planktonic foraminifera from the Gulf of Aden and the western tropical Indian Ocean, Deep Sea Drilling Project, Leg 24 in: Fisher, R.L.; Bunce, E.T., et al., Initial Reports of the Deep Sea Drilling Project, Volume 24, Washington (U.S. Government Printing Office), p. 827-850.

Zobel, B., 1974. Quaternary and Neogene Foraminifera: Biostratigraphy in: Simpson, E.S.W.; Schlich, R., et al., 1974, Initial Reports of the Deep Sea Drilling Project, Volume 25, Washington (U.S. Government Printing Office), p. 573-578.

Figure 2: Biostratigraphy, lithology and sample locations for DSDP Sites 231, 237, 249 and 360. Foram zones, as given in the Initial Reports of the Deep Sea Drilling Project are shown to the left of each lithologic column. Numbers within the lithologic columns refer to core numbers and numbers in parentheses are ages of datums in millions of years.

References for Figure 2

[1] Roth (1974)

[2] Burkry (1974)

[3] Muller (1974)

[4] Jenkins (1978)

[5] Decima, et al. (1974)

[6] Vincent, et al. (1974)

[7] Zobel (1974)

[8] Fisher, Bunce, et al. (1974)

[9] Simpson, Schlich, et al. (1974)

[10] Bolli, Ryan, et al. (1978)

[11] Ages in millions of years B.P., from Ryan, et al. (1974).

[12] Interpolated age in millions of years, assuming constant sedimentation rates

[13] Bukry (1973)

[14] Bukry (1975)

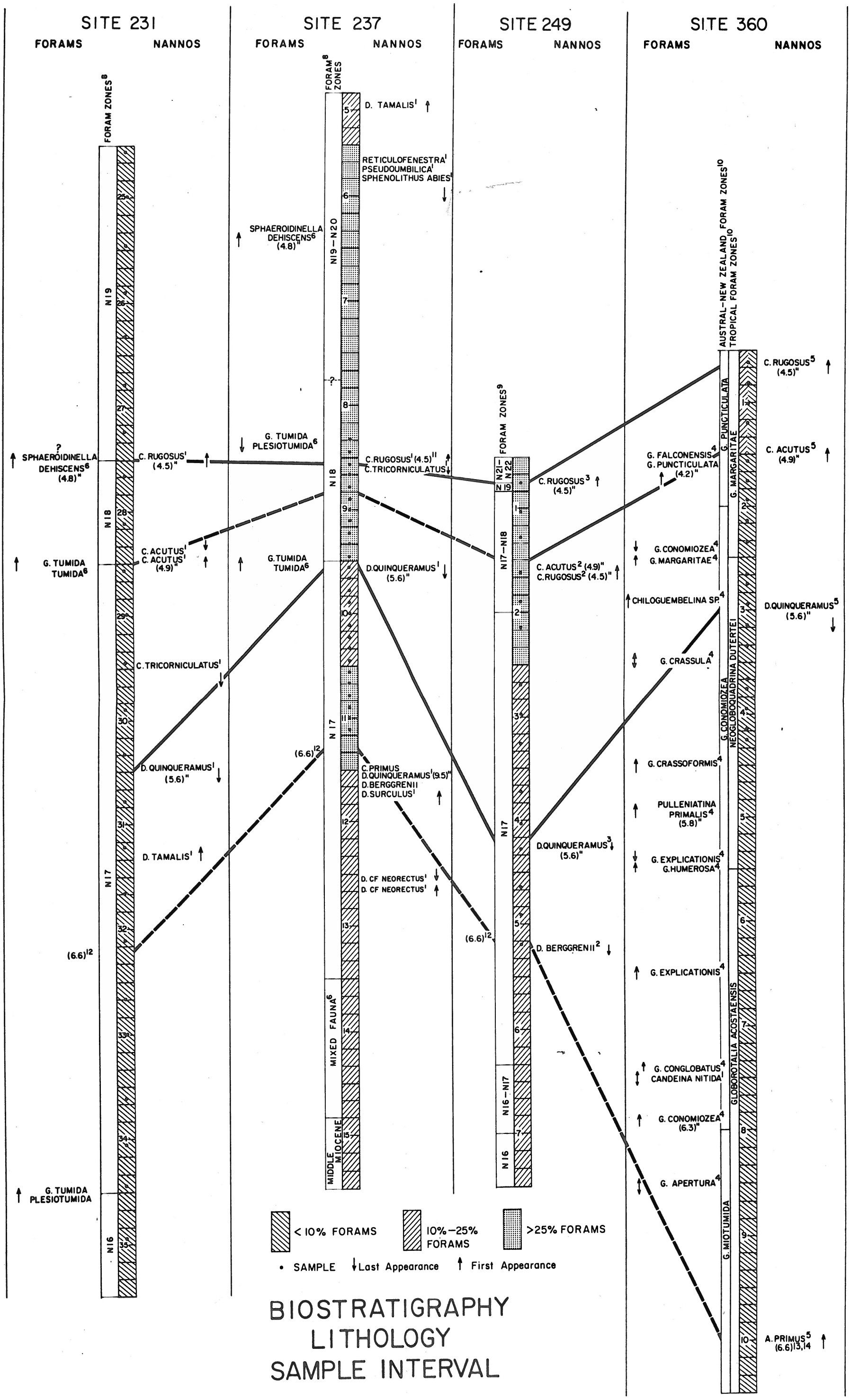
SITE 231
FORAMS
NANNOS
FORAM ZONES[8]
N19
N18
N17
N16
SITE 237
FORAMS
NANNOS
FORAM[8] ZONES
N19–N20
N18
N17
MIXED FAUNA[6]
MIDDLE MIOCENE
D. TAMALIS[1]
RETICULOFENESTRA[1] PSEUDOUMBILICA[1] SPHENOLITHUS ABIES[1]
SPHAEROIDINELLA DEHISCENS[6] (4.8)"
G. TUMIDA PLESIOTUMIDA[6]
C. RUGOSUS[1] (4.5)"
C. ACUTUS[1] C. ACUTUS[1] (4.9)"
G. TUMIDA TUMIDA[6]
C. TRICORNICULATUS[1]
D. QUINQUERAMUS[1] (5.6)"
(6.6)[12]
C. PRIMUS
D. QUINQUERAMUS[1] (9.5)"
D. BERGGRENII
D. SURCULUS[1]
D. CF NEORECTUS[1]
D. CF NEORECTUS[1]
SITE 249
FORAMS
NANNOS
FORAM ZONES[9]
N21–N22
N19
N17–N18
N17
N16–N17
N16
C. RUGOSUS[3] (4.5)"
C. ACUTUS[2] (4.9)"
C. RUGOSUS[2] (4.5)"
D. QUINQUERAMUS[3] (5.6)"
(6.6)[12]
D. BERGGRENII[2]
SITE 360
FORAMS
NANNOS
AUSTRAL–NEW ZEALAND FORAM ZONES[10]
TROPICAL FORAM ZONES[10]
G. PUNCTICULATA
G. MARGARITAE
G. CONOMIOZEA
NEOGLOBOQUADRINA DUTERTEI
GLOBOROTALIA ACOSTAENSIS
G. MIOTUMIDA
C. RUGOSUS[5] (4.5)"
G. FALCONENSIS[4] G. PUNCTICULATA (4.2)"
G. CONOMIOZEA[4] G. MARGARITAE[4]
CHILOGUEMBELINA SP.[4]
G. CRASSULA[4]
G. CRASSOFORMIS[4]
PULLENIATINA PRIMALIS[4] (5.8)"
G. EXPLICATIONIS[4] G. HUMEROSA[4]
G. EXPLICATIONIS[4]
G. CONGLOBATUS[4] CANDEINA NITIDA[1]
G. CONOMIOZEA[4] (6.3)"
G. APERTURA[4]
C. ACUTUS[5] (4.9)"
D. QUINQUERAMUS[5] (5.6)"
A. PRIMUS[5] (6.6)[13,14]
G. TUMIDA PLESIOTUMIDA
< 10% FORAMS
10%–25% FORAMS
>25% FORAMS
• SAMPLE
↓ Last Appearance
↑ First Appearance
BIOSTRATIGRAPHY
LITHOLOGY
SAMPLE INTERVAL